Physica D 400 (2019) 132158

Contents lists available at ScienceDirect

Physica D

journal homepage: www.elsevier.com/locate/physd

# Collective synchronization of the multi-component Gross–Pitaevskii–Lohe system ☆

Weizhu Bao [a], Seung-Yeal Ha [b,c], Dohyun Kim [d,*], Qinglin Tang [e]

[a] Department of Mathematics, National University of Singapore, Singapore, 119076, Singapore
[b] Department of Mathematical Sciences and Research Institute of Mathematics, Seoul National University, Seoul 08826, Republic of Korea
[c] Korea Institute for Advanced Study, Hoegiro 87, Seoul 02455, Republic of Korea
[d] National Institute for Mathematical Sciences, 70, Yuseong-daero 1689 beon-gil, Yuseong-gu, Daejeon 34047, Republic of Korea
[e] School of Mathematics, State Key Laboratory of Hydraulics and Mountain River Engineering, Sichuan University, Chengdu 610064, China

## HIGHLIGHTS

- Proposing a multi-component Gross–Pitaevskii–Lohe system which exhibits possible quantum synchronization phenomenon.
- Emergence of both synchronous behavior and periodic motion due to the identical and trapping harmonic potential.
- Presentation of sufficient conditions leading to the complete and practical synchronizations.
- Providing several numerical examples which support our theoretical results.

## ARTICLE INFO

*Article history:*
Received 12 March 2019
Received in revised form 5 July 2019
Accepted 19 July 2019
Available online 29 July 2019
Communicated by H. Nakao

*Keywords:*
Emergence
Kuramoto model
Nonlinear Schrödinger equation
Schrödinger–Lohe model
Time splitting
Quantum synchronization

## ABSTRACT

In this paper, we propose a multi-component Gross–Pitaevskii–Lohe (GPL for brevity) system in which quantum units interact with each other such that collective behaviors can emerge asymptotically. We introduce several sufficient frameworks leading to complete and practical synchronizations in terms of system parameters and initial data. For the modeling of interaction matrices we classify them into three types (fully identical, weakly identical and heterogeneous) and present emergent behaviors correspond to each interaction matrix. More precisely, for the fully identical case in which all components are same, we expect the emergence of the complete synchronization with exponential convergence rate. On the other hand for the remaining two interaction matrices, we can only show that the practical synchronization occurs under well-prepared initial frameworks. For instance, we assume that a coupling strength is sufficiently large and perturbation of an interaction matrix is sufficiently small. Regarding the practical synchronization estimates, due to the possible blow-up of a solution at infinity, we a priori assume that the $L^4$-norm of a solution is bounded on any finite time interval. In our analytical estimates, two-point correlation function approach will play a key role to derive synchronization estimates. We also provide several numerical simulations using time splitting Crank–Nicolson spectral method and compare them with our analytical results.



## 1. Introduction

After the first realization of the Bose–Einstein condensate (BEC) [1–3] for a trapped dilute Bosonic gas in 1995, the BEC has received considerable attention from mathematics and physics communities. Below a sufficiently low temperature smaller than the critical

☆ The authors acknowledge the support from Ministry of Education of Singapore grant R-146-000-247-114 (W. Bao), from the National Research Foundation of Korea (NRF-2017R1A5A1015626) (S.-Y. Ha), from the National Institute for Mathematical Sciences (NIMS) grant funded by the Korea government (MIST) (No.B19610000) (D. Kim) and from the Fundamental Research Funds for the Central Universities (YJ201807) (Q. Tang).

* Corresponding author.
*E-mail addresses:* matbaowz@nus.edu.sg (W. Bao), syha@snu.ac.kr (S.-Y. Ha), dohyunkim@nims.re.kr (D. Kim), qinglin_tang@scu.edu.cn (Q. Tang).
*URL:* http://www.math.nus.edu.sg/~bao/ (W. Bao).

https://doi.org/10.1016/j.physd.2019.132158
0167-2789/

temperature $T_c$, it is well known in [4,5] that the properties of the BEC are well described by the complex-valued wave function $\psi = \psi(x,t)$ whose governing dynamics is the Gross–Pitaevskii equation (GPE):

$$\mathrm{i}\partial_t \psi = -\frac{1}{2}\Delta\psi + V\psi + \beta|\psi|^2\psi, \quad x \in \mathbb{R}^d, \quad t > 0, \tag{1.1}$$

where $\mathrm{i} = \sqrt{-1}$ denotes the imaginary unit, and $V = V(x)$ and $\beta$ represent a real-valued trapping potential determined by the system and the short-time interaction rate, respectively. Several interesting properties of the BEC such as long-range dipole–dipole interaction, rotating frame and spin–orbit coupling can be considered both physically and mathematically (see [6] for a nice introduction for the BEC). From the numerics point of view, there are numerous developments to discretize GPE (1.1) via Crank–Nicolson finite difference (CNFD) method [6–9] and time-splitting sine pseudospectral method (TSSP) [6,10–14]. We also refer the reader to [7] as a review of numerical methods for nonlinear Schrödinger equations.

Recently, quantum synchronization attracts considerable interests from physics and engineering communities, especially in quantum optics, due to its potential application in quantum computing, quantum information and optomechanical control [15–27]. Moreover, there has been an attempt to link between classical synchronization and quantum entanglement [28]. See [29–31] for a brief introduction to classical synchronization. To date, several mathematical models were proposed to describe quantum synchronization, e.g., the quantum Van der Pol oscillator [32,33], quantum Liouville-type equations [34] and matrix-valued quantum Kuramoto model [35–38], etc. Among them, we are interested in synthesizing the M. Lohe's idea in [39–43] together with the GPE as a principle of modeling.

To fix the idea, we consider a quantum system whose components are distributed on each node, and $\psi_j = \psi_j(x,t)$ denotes the wave-function of the $j$th quantum sub-systems on the spatial domain $\mathbb{R}^d$. We assume that the dynamics of $\psi_j$ is governed by the multi-component Gross–Pitaevskii–Lohe system:

$$\begin{cases} \mathrm{i}\partial_t \psi_j = -\frac{1}{2}\Delta\psi_j + V_j\psi_j + \sum_{k=1}^{N}\beta_{jk}|\psi_k|^2\psi_j + \frac{\mathrm{i}\kappa}{2N}\sum_{k=1}^{N} a_{jk}\left(\psi_k - \frac{\langle\psi_j,\psi_k\rangle}{\langle\psi_j,\psi_j\rangle}\psi_j\right), \\ \psi_j(x,0) = \psi_j^0(x), \quad (x,t) \in \mathbb{R}^d \times \mathbb{R}_+, \quad j = 1,\dots,N. \end{cases} \tag{1.2}$$

For $\kappa = 0$, system (1.2) has been introduced as a model for multi-component model BEC [44–46] and/or spinor BEC [10,14,47]. Here, $V_j = V_j(x)$ is an external trapping potential acted on $j$th node, $\mathcal{B} = (\beta_{jk})$ takes account for the particle interaction rate where all $\beta_{jk}$ have positive values so that our system becomes defocusing, $\kappa$ represent a positive Lohe coupling strength and $\mathcal{A} = (a_{jk})$ describes the network structure between quantum sub-systems. Throughout the paper, we assume that the external potential $V_j$ has the form of quadratic function:

$$V_j(x) = \sum_{k=1}^{d}\frac{(\omega_j^k)^2}{2}|x^k|^2, \quad x = (x^1,\dots,x^d) \in \mathbb{R}^d, \quad \omega_j^k > 0 \quad \text{for all } j, k. \tag{1.3}$$

Global well-posedness for system (1.2) with (1.3) can be obtained using standard Strichartz estimate and energy estimate (see Theorem 3.1). In particular, global well-posedness theory yields that we have a uniform bound for $\psi_j$ in the $L^4$-norm in any finite-time interval. On the other hand, when Gross–Pitaevskii terms are zero, i.e., $\mathcal{B} = O$, system (1.2) becomes the Schrödinger–Lohe system whose emergent dynamics has been extensively studied in [34,40–43,48,49].

In this paper, we provide several sufficient frameworks leading to collective behaviors of the multi-component system (1.2). We denote the collective behaviors to describe emergent phenomena exhibiting the vanishing of difference between wave functions in some sense. More precisely, when the $L^2$-distances between all wave functions tend to zero, we call it "*complete synchronization*" (see Definition 3.1(i)). This is the case where external potentials are all identical. In contrast, when external potentials are distinct, it is most unlikely that the $L^2$-distances between wave functions tend to zero asymptotically (e.g., see Case 2 and Fig. 6.2(b)–(d) in Example 6.1). Hence we cannot expect the complete synchronization. Thus, we need to introduce a weak concept of synchronization, namely "*practical synchronization*" to denote the situation that we can make the $L^2$-distances small by tuning the Lohe coupling strength $\kappa$ large enough (see Definition 3.1(ii)).

The main results of this paper are two-fold. First, we deal with a two-component system with $N = 2$ and identical harmonic potential as an external potential. When the interaction matrix $\mathcal{B} = (\beta_{ij})$ is a positive constant multiple of $J_2$ (where all entries are one), our first result says that the complete synchronization occurs asymptotically and center-of-mass tends to harmonic motion asymptotically (see Theorem 3.2). Second, we deal with a multi-component system with $N \geq 3$ under three types of coupling matrices (fully identical, weakly identical and heterogeneous). More precisely, we consider the following three cases in terms of the interaction matrix $\mathcal{B} = (\beta_{ij})$:

(i) (Fully identical interaction) : $\mathcal{B} = \beta\mathbf{J}_N$,

where $\mathbf{J}_N$ denotes the $N \times N$ matrix whose components are all 1.

(ii) (Weakly identical interaction) : $\mathcal{B} = \beta\mathbf{J}_N + \mathrm{diag}(\varepsilon_1,\dots,\varepsilon_N)$.

(iii) (heterogeneous interaction) : $\mathcal{B} = \begin{pmatrix} \beta & \beta_{12} & \cdots & \beta_{1N} \\ \beta_{21} & \beta & \cdots & \beta_{2N} \\ \vdots & \vdots & \ddots & \vdots \\ \beta_{N1} & \beta_{N2} & \cdots & \beta \end{pmatrix} + \mathrm{diag}(\varepsilon_1,\dots,\varepsilon_N)$.

For the fully identical case, if the relative distances between initial data are small, the Lohe coupling strength is positive and the network topology $\mathcal{A} =: (a_{ij})$ is close to the identity matrix in $L^\infty$ sense (see the condition (3.6)), the complete synchronization occurs exponentially fast (see Theorem 3.3), i.e., there exists a positive constant $\alpha$ depending only on the network structure $\mathcal{A}$ such that

$$\max_{1\leq i,j\leq N}\|\psi_i(t) - \psi_j(t)\|_{L^2(\mathbb{R}^d)} \leq \mathcal{O}(1)e^{-\alpha t}, \quad t \geq 0.$$

On the other hand, for the weakly identical and heterogeneous cases, we impose several initial conditions on the system parameters. For instance, as in the identical case, the network topology is close to the identity matrix in $L^\infty$-norm. This is realized as $\lambda(\mathcal{A}) > 0$ in Theorems 3.4 and 3.5. For the interaction matrix $\mathcal{B}$, its perturbation from the identity matrix is sufficiently small and for the coupling strength $\kappa$, it should be sufficiently large and we provide its lower bound, which would not be optimal, in (3.7) and (3.10). To be more specific, we control the maximal $L^2$-distance between wavefunctions in terms of $1/\kappa$ so that we are able to make the maximal $L^2$-distance small as we wish by controlling the coupling strength. On the other hand, due to the possible blow-up of the $L^4$-norms of a global solution at $t \to \infty$, we do not provide the uniform-in-time practical synchronization estimate. Note that since the $L^4$-estimate is not required in the identical case, we can present the uniform-in-time estimate which is valid on $t \to \infty$. Hence, when we deal with the weakly identical and heterogeneous cases, we alternatively consider the estimates valid on any finite time interval. To this end, we derive practical synchronization estimates on any finite-time interval: for $T > 0$,

$$\sup_{0\le t\le T} \max_{1\le i,j\le N} \|\psi_i(t) - \psi_j(t)\|_{L^2(\mathbb{R}^d)} \le \mathcal{O}\left(\frac{1}{\sqrt{\kappa}}\right),$$

under suitable assumptions on the network structure and large coupling strength (see Theorems 3.4 and 3.5).

The rest of the paper is organized as follows. In Section 2, we study a priori estimates for the multi-component GPL system and derive the dynamics of the mass, energy and two-point correlation function. We also briefly discuss the relation with other synchronization models. In Section 3, we present our two main results on the two-component system and multi-component system. In Section 4, we provide the proof of the two-component system. More precisely, we show that for generic initial data, complete synchronization and periodic harmonic motion can arise simultaneously. In Section 5, for the multi-component system, we present two frameworks leading to the practical synchronization. In Section 6, we provide several numerical simulations and compare them with our analytical results. Finally, Section 7 is devoted to a summary of our main results and some remaining issues for future works. In Appendix A, we present a proof of Theorem 3.1, and in Appendix B, we provide a proof of Lemma 4.3.

**Notation**: Let $f$ and $g$ be complex-valued functions defined on $\mathbb{R}^d$ and $p \in [1,\infty]$. Then, we set $L^p$-norm of $f$ as $\|f\|_p$. In particular, we denote the inner product and $L^2$-norm as follows:

$$\langle f, g\rangle := \int_{\mathbb{R}^d} f(x)\bar{g}(x)dx, \quad \|f\| := \sqrt{\langle f, f\rangle},$$

where $\bar{g}$ denotes the complex conjugate of $g$. For given finite sequences $(p_i)$, $(p_{ij})$ in $\mathbb{R}^N$ and $\mathbb{R}^{N\times N}$, we set

$$\max_i p_i := \max_{1\le i\le N} p_i, \quad \min_i p_i := \min_{1\le i\le N} p_i, \quad \max_{k,l} p_{kl} := \max_{1\le k,l\le N} p_{kl}, \quad \min_{k,l} p_{kl} := \min_{1\le k,l\le N} p_{kl}.$$

## 2. Preliminaries

In this section, we study a priori estimates for the multi-component Gross–Pitaevskii–Lohe (GPL) system and relations with other existing models for synchronization.

### 2.1. The Gross–Pitaevskii–Lohe system

Consider the Cauchy problem for the GPL system:

$$\begin{cases} \mathrm{i}\partial_t\psi_j = -\frac{1}{2}\Delta\psi_j + V_j\psi_j + \sum_{k=1}^N \beta_{jk}|\psi_k|^2\psi_j + \frac{\mathrm{i}\kappa}{2N}\sum_{k=1}^N a_{jk}\left(\psi_k - \frac{\langle\psi_j,\psi_k\rangle}{\langle\psi_j,\psi_j\rangle}\psi_j\right), \\ \psi_j(x,0) = \psi_j^0(x), \quad (x,t)\in\mathbb{R}^d\times\mathbb{R}_+, \quad j = 1,\dots,N. \end{cases} \tag{2.1}$$

Note that when we turn off the Lohe coupling with $\kappa = 0$, system (2.1) reduces to the multi-component Gross–Pitaevskii system [44–46] for BEC:

$$\mathrm{i}\partial_t\psi_j = -\frac{1}{2}\Delta\psi_j + V_j\psi_j + \sum_{k=1}^N \beta_{jk}|\psi_k|^2\psi_j, \quad t > 0, \quad j = 1,\dots,N.$$

In contrast, when we set $\beta_{jk} \equiv 0$ in system (2.1), system (2.1) reduces to the Schrödinger–Lohe model for quantum synchronization which has been introduced in [50]:

$$\mathrm{i}\partial_t\psi_j = -\frac{1}{2}\Delta\psi_j + V_j\psi_j + \frac{\mathrm{i}\kappa}{2N}\sum_{k=1}^N a_{jk}\left(\psi_k - \frac{\langle\psi_j,\psi_k\rangle}{\langle\psi_j,\psi_j\rangle}\psi_j\right), \quad t > 0, \quad j = 1,\dots,N.$$

Hence, the GPL system contains two quantum mechanical phenomena: the Bose–Einstein condensation and the quantum synchronization.

Now, we look for the relation with classical synchronization models. To see the relation, we need to set ansätze for $V_j$ and $\psi_j$:

$$V_j(x) = \upsilon_j \in \mathbb{R} : \text{constant}, \quad \psi_j(x,t) := e^{-\mathrm{i}\theta_j(t)}, \quad (x,t)\in\mathbb{R}^d\times\mathbb{R}_+.$$

We substitute the ansätze above into $(2.1)_1$ to get

$$\dot{\theta}_j e^{-\mathrm{i}\theta_j} = \left(\sum_{k=1}^N \beta_{jk} + \upsilon_j\right)e^{-\mathrm{i}\theta_j} + \frac{\mathrm{i}\kappa}{2N}\sum_{k=1}^N a_{ik}\left(e^{-\mathrm{i}\theta_k} - e^{-\mathrm{i}(\theta_j-\theta_k)}e^{-\mathrm{i}\theta_j}\right). \tag{2.2}$$

We multiply the relation (2.2) with $e^{\mathrm{i}\theta_j}$ and take real parts in both sides to find the Kuramoto model [51]:

$$\dot{\theta}_j = \nu_j + \frac{\kappa}{N}\sum_{k=1}^{N}\sin(\theta_k - \theta_j), \quad \nu_j := \sum_{k=1}^{N}\beta_{jk} + v_j.$$

Thus, the GPL system incorporates the quantum and classical synchronous features.

### 2.2. A priori estimates

In this subsection, we study a priori estimates such as the $L^2$-conservation and dissipative energy estimate.

For $\Psi = (\psi_1, \ldots, \psi_N)$, we introduce an energy functional $\mathcal{E}[\Psi]$ and energy production terms as follows:

$$\begin{aligned}
&\mathcal{E}_j^1[\Psi] := \int_{\mathbb{R}^d}\left[\frac{1}{2}|\nabla\psi_j|^2 + V_j|\psi_j|^2 + \frac{1}{2}\sum_{k=1}^{N}\beta_{jk}|\psi_k|^2|\psi_j|^2\right]dx, \quad j = 1,\ldots,N,\\
&\mathcal{E}_j^2[\Psi] := \int_{\mathbb{R}^d}\Bigg[\frac{1}{2}|\nabla\psi_j|^2 + \frac{1}{4N}\sum_{k=1}^{N}(V_j + V_k)(|\psi_j|^2 + |\psi_k|^2)\\
&\qquad\qquad + \frac{1}{8N}\sum_{k,\ell=1}^{N}(\beta_{j\ell} + \beta_{k\ell})|\psi_\ell|^2(|\psi_j|^2 + |\psi_k|^2)\Bigg]dx,\\
&r_j^{\mathrm{av}}(t) := \frac{1}{N}\sum_{k=1}^{N}\mathrm{Re}\langle\psi_j, \psi_k\rangle, \quad \mathcal{E}[\Psi] := \sum_{j=1}^{N}\mathcal{E}_j^1[\Psi],\\
&\mathcal{E}_{\mathrm{d}}[\Psi] := \frac{\kappa}{4N}\sum_{j,k=1}^{N}\int_{\mathbb{R}^d}|\nabla\psi_k - \nabla\psi_j|^2\,dx + \int_{\mathbb{R}^d}(V_j + V_k)|\psi_j - \psi_k|^2\,dx\\
&\qquad + \frac{\kappa}{8N}\sum_{j,k,\ell=1}^{N}\int_{\mathbb{R}^d}(\beta_{j\ell} + \beta_{k\ell})|\psi_j - \psi_k|^2\,dx.
\end{aligned} \tag{2.3}$$

**Remark 2.1.** $\mathcal{E}_j^1[\Psi]$ is the energy of $j$th wavefunction, and it is well-known that the energy $\mathcal{E}_j^1[\Psi]$ is conserved for $\kappa = 0$ and each $j = 1,\ldots,N$. On the other hand, $\mathcal{E}_j^2[\Psi]$ measures how oscillators are far from the identical state. More precisely, for the identical external potentials and interaction rates:

$$V_j \equiv V, \quad \mathcal{B} = \beta J_N,$$

it follows from (A.4) that

$$\sum_{j=1}^{N}\mathcal{E}_j^1[\Psi] = \sum_{j=1}^{N}\mathcal{E}_j^2[\Psi].$$

Finally, $\mathcal{E}_d[\Psi]$ describes the total energy difference between wavefunctions.

In the following lemma, we show that $L^2$-conservation of $\psi_j$ and energy estimates. However, we see that the total energy would not be conserved along the GPL flow.

**Lemma 2.1.** *Let $\psi_j$ be a global smooth solution to (2.1) with the following conditions:*

$$\|\psi_j^0\| = 1, \quad \text{for all } j = 1,\ldots,N \quad \text{and} \quad \mathcal{A} = J_N.$$

*Then, we have*

$$\frac{d}{dt}\|\psi_j\|^2 = 0, \quad j = 1,\ldots,N, \quad \frac{d}{dt}\mathcal{E}[\Psi] = \kappa\sum_{j=1}^{N}\mathcal{E}_j^2[\Psi] - \kappa\sum_{j=1}^{N}r_j\mathcal{E}_j^1[\Psi] - \kappa\mathcal{E}_d[\Psi], \quad t > 0.$$

**Proof.** (i) The $L^2$-conservation is rather straightforward. Thus, we omit its details.
(ii) Since the energy in relation (2.3) is conserved for the case $\kappa = 0$, we only need to focus on the term containing the Lohe coupling strength $\kappa$. Note that the following relation holds:

$$\partial_t|\psi_j|^2 = \partial_t\Big(\psi_j\bar{\psi}_j\Big) = (\partial_t\psi_j)\bar{\psi}_j + \psi_j\overline{\partial_t\psi_j} = \overline{\overline{\partial_t\psi_j}\psi_j} + \overline{\partial_t\psi_j}\psi_j = 2\mathrm{Re}\Big(\partial_t\psi_j\cdot\bar{\psi}_j\Big). \tag{2.4}$$

By integration by parts, we have

$$\begin{aligned}
\frac{d}{dt}\mathcal{E}[\Psi] &= \sum_{j=1}^{N}\int_{\mathbb{R}^d}\partial_t\left(-\frac{1}{2}\bar{\psi}_j\Delta\psi_j\right) + \partial_t\Big(V_j\bar{\psi}_j\psi_j\Big) + \partial_t\left(\frac{1}{2}\sum_{\ell=1}^{N}\beta_{j\ell}|\psi_\ell|^2\bar{\psi}_j\psi_j\right)\\
&= \sum_{j=1}^{N}\int_{\mathbb{R}^d}\mathrm{Re}\left[\partial_t\psi_j\left(-\frac{1}{2}\Delta\bar{\psi}_j + V_j\bar{\psi}_j + \frac{1}{2}\sum_{\ell=1}^{N}\beta_{j\ell}|\psi_\ell|^2\bar{\psi}_j\right)\right]dx
\end{aligned}$$

$$
\begin{aligned}
&= \frac{\kappa}{N}\sum_{j=1}^{N}\int_{\mathbb{R}^d} \mathrm{Re}\left[\left(\sum_{k=1}^{N}\psi_k - \langle \psi_j, \psi_k\rangle \psi_j\right)\left(-\frac{1}{2}\Delta\bar{\psi}_j + V_j\bar{\psi}_j + \frac{1}{2}\sum_{\ell=1}^{N}\beta_{j\ell}|\psi_\ell|^2\bar{\psi}_j\right)\right]dx \\
&= \frac{\kappa}{N}\sum_{j,k=1}^{N}\int_{\mathbb{R}^d} \mathrm{Re}\left[-\frac{1}{2}\psi_k\Delta\bar{\psi}_j + V_j\psi_k\bar{\psi}_j + \frac{1}{2}\sum_{\ell=1}^{N}\beta_{j\ell}|\psi_\ell|^2\psi_k\bar{\psi}_j\right]dx \\
&\qquad - \frac{\kappa}{N}\sum_{j,k=1}^{N} \mathrm{Re}\left[\langle \psi_j, \psi_k\rangle \int_{\mathbb{R}^d}\left(-\frac{1}{2}\psi_j\Delta\bar{\psi}_j + V_j|\psi_j|^2 + \frac{1}{2}\sum_{\ell=1}^{N}\beta_{j\ell}|\psi_\ell|^2|\psi_j|^2\right)dx\right] \\
&=: \mathcal{I}_{11} + \mathcal{I}_{12}.
\end{aligned}
\tag{2.5}
$$

Below, we present estimates of $\mathcal{I}_{11}$ and $\mathcal{I}_{12}$, respectively.

• (Estimate of $\mathcal{I}_{11}$): For the notational simplicity, we set

$$
C_j[\Psi] := \frac{1}{2}\sum_{\ell=1}^{N}\beta_{j\ell}|\psi_\ell|^2 \in \mathbb{R}, \quad j = 1, \dots, N. \tag{2.6}
$$

Then, we split the term $\mathcal{I}_{11}$ into two terms:

$$
\begin{aligned}
\mathcal{I}_{11} &= \frac{\kappa}{N}\sum_{j,k=1}^{N}\int_{\mathbb{R}^d} \mathrm{Re}\left[-\frac{1}{2}\psi_k\Delta\bar{\psi}_j + V_j\psi_k\bar{\psi}_j + \frac{1}{2}\sum_{\ell=1}^{N}\beta_{j\ell}|\psi_\ell|^2\psi_k\bar{\psi}_j\right]dx \\
&= \frac{\kappa}{N}\sum_{j,k=1}^{N}\int_{\mathbb{R}^d} \mathrm{Re}\left[-\frac{1}{2}\psi_k\Delta\bar{\psi}_j + (V_j + C_j[\Psi])\psi_k\bar{\psi}_j\right]dx \\
&=: \mathcal{I}_{111} + \mathcal{I}_{112}.
\end{aligned}
\tag{2.7}
$$

◇ (Estimate of $\mathcal{I}_{111}$): We use the following identity:

$$
2\mathrm{Re}(u\cdot\bar{v}) = |u|^2 + |v|^2 - |u-v|^2 \quad \text{for } u, v \in \mathbb{C}^d, \tag{2.8}
$$

to find

$$
\begin{aligned}
\mathcal{I}_{111} &= \frac{\kappa}{N}\sum_{j,k=1}^{N}\int_{\mathbb{R}^d} \mathrm{Re}\left[-\frac{1}{2}\psi_k\Delta\bar{\psi}_j\right]dx = \frac{\kappa}{N}\sum_{j,k=1}^{N}\int_{\mathbb{R}^d} \mathrm{Re}\left[\frac{1}{2}\nabla\psi_k\cdot\nabla\bar{\psi}_j\right]dx \\
&= \frac{\kappa}{N}\sum_{j,k=1}^{N}\int_{\mathbb{R}^d} \frac{1}{4}\Big(|\nabla\psi_k|^2 + |\nabla\psi_j|^2 - |\nabla\psi_k - \nabla\psi_j|^2\Big)dx \\
&= \frac{\kappa}{2}\sum_{j=1}^{N}\int_{\mathbb{R}^d}|\nabla\psi_j|^2dx - \frac{\kappa}{4N}\sum_{j,k=1}^{N}\int_{\mathbb{R}^d}|\nabla\psi_k - \nabla\psi_j|^2\,dx.
\end{aligned}
\tag{2.9}
$$

◇ (Estimate of $\mathcal{I}_{112}$): We use the index change trick $j \leftrightarrow k$ and the identity (2.8) to see

$$
\begin{aligned}
\mathcal{I}_{112} &= \frac{\kappa}{N}\sum_{j,k=1}^{N}\int_{\mathbb{R}^d} \mathrm{Re}\Big[(V_j + C_j[\Psi])\psi_k\bar{\psi}_j\Big]dx \\
&= \frac{\kappa}{2N}\sum_{j,k=1}^{N}\int_{\mathbb{R}^d} \mathrm{Re}\Big[(V_j + C_j[\Psi])\psi_k\bar{\psi}_j + (V_k + C_k[\Psi])\psi_j\bar{\psi}_k\Big]dx \\
&= \frac{\kappa}{2N}\sum_{j,k=1}^{N}\int_{\mathbb{R}^d} \mathrm{Re}\Big[(V_j + C_j[\Psi] + V_k + C_k[\Psi])\psi_k\bar{\psi}_j\Big]dx \\
&= \frac{\kappa}{4N}\sum_{j,k=1}^{N}\int_{\mathbb{R}^d}(V_j + V_k + C_j[\Psi] + C_k[\Psi])(|\psi_k|^2 + |\psi_j|^2 - |\psi_j - \psi_k|^2)dx \\
&= \frac{\kappa}{4N}\sum_{j,k=1}^{N}\int_{\mathbb{R}^d}(V_j + V_k)(|\psi_k|^2 + |\psi_j|^2)\,dx + \frac{\kappa}{4N}\sum_{j,k=1}^{N}\int_{\mathbb{R}^d}(C_j[\Psi] + C_k[\Psi])(|\psi_k|^2 + |\psi_j|^2)\,dx \\
&\qquad - \frac{\kappa}{4N}\sum_{j,k=1}^{N}\int_{\mathbb{R}^d}(V_j + V_k + C_j[\Psi] + C_k[\Psi])|\psi_j - \psi_k|^2\,dx.
\end{aligned}
\tag{2.10}
$$

In (2.7), it follows from (2.9) and (2.10) that

$$
\begin{aligned}
\mathcal{I}_{11} &= \frac{\kappa}{2}\sum_{j=1}^{N}\int_{\mathbb{R}^d}|\nabla\psi_j|^2dx + \frac{\kappa}{4N}\sum_{j,k=1}^{N}\int_{\mathbb{R}^d}(V_j+V_k)(|\psi_k|^2+|\psi_j|^2)\,dx \\
&\quad + \frac{\kappa}{4N}\sum_{j,k=1}^{N}\int_{\mathbb{R}^d}(C_j[\Psi]+C_k[\Psi])(|\psi_k|^2+|\psi_j|^2)\,dx - \frac{\kappa}{4N}\sum_{j,k=1}^{N}\int_{\mathbb{R}^d}|\nabla\psi_k-\nabla\psi_j|^2\,dx \\
&\quad - \frac{\kappa}{4N}\sum_{j,k=1}^{N}\int_{\mathbb{R}^d}(V_j+V_k+C_j[\Psi]+C_k[\Psi])|\psi_j-\psi_k|^2\,dx.
\end{aligned} \tag{2.11}
$$

• (Estimate of $\mathcal{I}_{12}$) By straightforward calculation, one has

$$
\begin{aligned}
\mathcal{I}_{12} &= -\frac{\kappa}{N}\sum_{j,k=1}^{N}\mathrm{Re}\left[\langle\psi_j,\psi_k\rangle\int_{\mathbb{R}^d}\left(-\frac{1}{2}\psi_j\Delta\bar{\psi}_j+(V_j+C_j[\Psi])|\psi_j|^2dx\right)\right] \\
&= -\frac{\kappa}{N}\sum_{j,k=1}^{N}\mathrm{Re}\left[\langle\psi_j,\psi_k\rangle\int_{\mathbb{R}^d}\frac{1}{2}|\nabla\psi_j|^2+(V_j+C_j[\Psi])|\psi_j|^2\,dx\right] \\
&= -\kappa\sum_{j=1}^{N}r_j\int_{\mathbb{R}^d}\frac{1}{2}|\nabla\psi_j|^2+V_j|\psi_j|^2+C_j[\Psi]|\psi_j|^2\,dx.
\end{aligned} \tag{2.12}
$$

In (2.5), we combine (2.11) and (2.12) to obtain the desired energy estimate:

$$
\frac{d}{dt}\mathcal{E}[\Psi] = \kappa\sum_{j=1}^{N}\mathcal{E}_j^2[\Psi] - \kappa\sum_{j=1}^{N}r_j\mathcal{E}_j^1[\Psi] - \kappa\mathcal{E}_{\mathrm{d}}[\Psi], \quad t>0. \tag{2.13}
$$

Note that we do not have definite monotonicity of the energy functional. □

Next, we introduce our key quantity "two-point correlation functions" for synchronization estimates as follows:

$$
h_{ij} := \langle\psi_i,\psi_j\rangle, \quad d_i^{\mathrm{av}}(\mathcal{A}) := \frac{1}{N}\sum_{j=1}^{N}a_{ij}, \quad i,j=1,\dots,N.
$$

**Lemma 2.2.** *Let $\psi_j$ be a global smooth solution to (1.2) with $\|\psi_j^0\|=1$ for $j=1,\dots,N$. Then, for $t>0$ and $i,j=1,\dots,N$, one has*

$$
\begin{aligned}
\frac{d}{dt}(1-h_{ij}) &= \mathrm{i}\int_{\mathbb{R}^d}(V_i-V_j)\psi_i\bar{\psi}_jdx \\
&+\mathrm{i}\int_{\mathbb{R}^d}\Big((\beta_{ji}-\beta_{ii})|\psi_i|^2+(\beta_{jj}-\beta_{ij})|\psi_j|^2+\sum_{k\neq i,j}(\beta_{ik}-\beta_{jk})|\psi_k|^2\Big)\psi_i\bar{\psi}_jdx \\
&-\frac{\kappa}{2}(d_i^{av}(\mathcal{A})+d_j^{av}(\mathcal{A}))(1-h_{ij}) \;+\frac{\kappa}{2N}\sum_{k=1}^{N}\Big(a_{ik}(1-h_{ik})(1-h_{ij})+a_{jk}(1-h_{kj})(1-h_{ij}) \\
&\qquad\qquad +(a_{ik}-a_{jk})(1-h_{kj}-(1-h_{ik}))\Big).
\end{aligned} \tag{2.14}
$$

**Proof.** We use $(1.2)_1$ to get

$$
\begin{aligned}
\frac{d}{dt}\langle\psi_i,\psi_j\rangle &= \langle\partial_t\psi_i,\psi_j\rangle+\langle\psi_i,\partial_t\psi_j\rangle \\
&= \left(\frac{\mathrm{i}}{2}\langle\Delta\psi_i,\psi_j\rangle-\frac{\mathrm{i}}{2}\langle\psi_i,\Delta\psi_j\rangle\right)+\Big(-\mathrm{i}\langle V_i\psi_i,\psi_j\rangle+\mathrm{i}\langle\psi_i,V_j\psi_j\rangle\Big) \\
&\quad -\mathrm{i}\sum_{k=1}^{N}\Big(\langle\beta_{ik}|\psi_k|^2\psi_i,\psi_j\rangle+\mathrm{i}\langle\psi_i,\beta_{jk}|\psi_k|^2\psi_j\rangle\Big) \\
&\quad +\frac{\kappa}{2N}\sum_{k=1}^{N}a_{ik}\langle\psi_k-h_{ik}\psi_i,\psi_j\rangle+a_{jk}\langle\psi_i,\psi_k-h_{jk}\psi_j\rangle \\
&=: \mathcal{I}_{21}+\mathcal{I}_{22}+\mathcal{I}_{23}+\mathcal{I}_{24}.
\end{aligned}
$$

In what follows, we present the estimates for $\mathcal{I}_{2k},\ k=1,2,3,4$, separately.

• (Estimate of $\mathcal{I}_{21}$): We use the self-adjoint property of the Laplacian to see

$$
\mathcal{I}_{21} = \frac{\mathrm{i}}{2}\langle\Delta\psi_i,\psi_j\rangle-\frac{\mathrm{i}}{2}\langle\psi_i,\Delta\psi_j\rangle = \frac{\mathrm{i}}{2}\langle\psi_i,\Delta\psi_j\rangle-\frac{\mathrm{i}}{2}\langle\psi_i,\Delta\psi_j\rangle = 0.
$$

• (Estimate of $\mathcal{I}_{22}$): Since $V_i$ is real-valued, one has

$$\mathcal{I}_{22} = -\mathrm{i}\langle V_i\psi_i, \psi_j\rangle + \mathrm{i}\langle \psi_i, V_j\psi_j\rangle = \mathrm{i}\int_{\mathbb{R}^d}(V_j - V_i)\psi_i\bar{\psi}_j\,dx.$$

• (Estimate of $\mathcal{I}_{23}$): We split the term $\mathcal{I}_{23}$ into several terms to find

$$\begin{aligned}
\mathcal{I}_{23} &= \sum_{k=1}^{N}\left\langle -\mathrm{i}\beta_{ik}|\psi_k|^2\psi_i, \psi_j\right\rangle + \mathrm{i}\left\langle \psi_i, \beta_{jk}|\psi_k|^2\psi_j\right\rangle \\
&= -\mathrm{i}\langle \beta_{ii}|\psi_i|^2\psi_i, \psi_j\rangle - \mathrm{i}\langle \beta_{ij}|\psi_j|^2\psi_i, \psi_j\rangle - \mathrm{i}\sum_{k\neq i,j}^{N}\langle \beta_{ik}|\psi_k|^2\psi_i, \psi_j\rangle \\
&\quad + \mathrm{i}\langle \psi_i, \beta_{ji}|\psi_i|^2\psi_j\rangle + \mathrm{i}\langle \psi_i, \beta_{jj}|\psi_j|^2\psi_j\rangle + \mathrm{i}\sum_{k\neq i,j}^{N}\langle \psi_i, \beta_{jk}|\psi_k|^2\psi_j\rangle \\
&= \mathrm{i}(\beta_{ji} - \beta_{ii})\int_{\mathbb{R}^d}|\psi_i|^2\psi_i\bar{\psi}_j\,dx + \mathrm{i}(\beta_{jj} - \beta_{ij})\int_{\mathbb{R}^d}|\psi_j|^2\psi_i\bar{\psi}_j\,dx \\
&\quad + \mathrm{i}\sum_{k\neq i,j}(\beta_{jk} - \beta_{ik})\int_{\mathbb{R}^d}|\psi_k|^2\psi_i\bar{\psi}_j\,dx.
\end{aligned}$$

• (Estimate of $\mathcal{I}_{24}$): We recall a definition of the two-point correlation function $h_{ij}$ to see

$$\begin{aligned}
\mathcal{I}_{24} &= \frac{\kappa}{2N}\sum_{k=1}^{N}\Big[a_{ik}\langle \psi_k - h_{ik}\psi_i, \psi_j\rangle + a_{jk}\langle \psi_i, \psi_k - h_{jk}\psi_j\rangle\Big] \\
&= \frac{\kappa}{2N}\sum_{k=1}^{N}\Big[a_{ik}(h_{kj} - h_{ik}h_{ij}) + a_{jk}(h_{ik} - h_{kj}h_{ij})\Big] \\
&= \frac{\kappa}{2N}\sum_{k=1}^{N}\Big[a_{ik}h_{ik}(1 - h_{ij}) + a_{ik}(h_{kj} - h_{ik}) + a_{jk}h_{kj}(1 - h_{ij}) + a_{jk}(h_{ik} - h_{kj})\Big] \\
&= \frac{\kappa}{2N}\sum_{k=1}^{N}\Big[\big(a_{ik}(h_{ik} - 1) + a_{jk}(h_{kj} - 1)\big)(1 - h_{ij}) + (a_{ik} + a_{jk})(1 - h_{ij}) \\
&\qquad\qquad + (a_{ik} - a_{jk})(h_{kj} - h_{ik})\Big].
\end{aligned}$$

Finally, we combine all estimates to find the desired dynamics. □

As a direct application of Lemma 2.2, we can derive cross-ratio like quantities which play a key role in the selection of possible asymptotic states:

$$\mathcal{R}_{ijk\ell} := \frac{(1 - h_{ij})(1 - h_{k\ell})}{(1 - h_{i\ell})(1 - h_{kj})}, \quad 1 \le i, j, k, \ell \le N. \tag{2.15}$$

In fact, authors of [49] showed that the quantities above are conserved along the GPL system with $\mathcal{B} = O$ and $\mathcal{A} = J_N$. Here, we also show that this quantity is conserved along the flow (1.2) provided that $\mathcal{A} = J_N$ and $\mathcal{B} = \beta J_N$.

**Corollary 2.1.** *Suppose that the initial data, the interaction matrix $\mathcal{B}$, network topology $\mathcal{A}$ and external potentials satisfy*

$$\mathcal{A} = J_N, \quad \mathcal{B} = \beta J_N, \quad \|\psi_j^0\| = 1, \quad V_j \equiv V, \quad j = 1, \ldots, N, \tag{2.16}$$

*and let $\psi_j$ be a smooth global solution to (1.2). Then, $\mathcal{R}_{ijk\ell}$ is invariant under the flow (2.1).*

**Proof.** We substitute (2.16) into (2.14) to see

$$\begin{aligned}
\frac{d}{dt}(1 - h_{ij}) &= -\frac{\kappa}{2N}\sum_{k=1}^{N}(h_{ik} + h_{kj})(1 - h_{ij}) \\
&= -\kappa(1 - h_{ij})(\langle \psi_i, \zeta\rangle + \langle \zeta, \psi_j\rangle), \quad \zeta := \frac{1}{2N}\sum_{k=1}^{N}\psi_k.
\end{aligned}$$

This yields

$$\frac{(1 - h_{ij})'}{1 - h_{ij}} = -\kappa(\langle \psi_i, \zeta\rangle + \langle \zeta, \psi_j\rangle). \tag{2.17}$$

On the other hand, it follows from (2.15) that

$$\ln \mathcal{R}_{ijk\ell} = \ln(1 - h_{ij}) + \ln(1 - h_{k\ell}) - \ln(1 - h_{i\ell}) - \ln(1 - h_{kj}).$$

Finally, we differentiate the relation above and use (2.17) to obtain

$$\begin{aligned}\frac{d}{dt}\ln \mathcal{R}_{ijk\ell} &= \frac{(1-h_{ij})'}{1-h_{ij}} + \frac{(1-h_{k\ell})'}{1-h_{k\ell}} - \frac{(1-h_{i\ell})'}{1-h_{i\ell}} - \frac{(1-h_{kj})'}{1-h_{kj}} \\ &= -\kappa(\langle\psi_i,\zeta\rangle + \langle\zeta,\psi_j\rangle) - \kappa(\langle\psi_k,\zeta\rangle + \langle\zeta,\psi_\ell\rangle) \\ &\quad + \kappa(\langle\psi_i,\zeta\rangle + \langle\zeta,\psi_\ell\rangle) + \kappa(\langle\psi_k,\zeta\rangle + \langle\zeta,\psi_j\rangle) \\ &= 0. \quad \square\end{aligned}$$

## 3. Description of main results

In this section, we briefly discuss our main results in the collective synchronous behaviors of the GPL system. First, we recall definitions of complete and practical synchronizations as follows.

**Definition 3.1.** Let $\psi_j$ be a solution to (1.2) and $T \in (0,\infty)$.

(1) System (1.2) exhibits complete synchronization, if $L^2$-distances between wave functions tend to zero asymptotically:

$$\lim_{t\to\infty}\max_{i,j}\|\psi_i(t)-\psi_j(t)\| = 0.$$

(2) System (1.2) exhibits practical synchronization in finite time interval $[0,T]$, if

$$\lim_{\kappa\to+\infty}\sup_{0\le t\le T}\max_{i,j}\|\psi_i(t)-\psi_j(t)\| = 0.$$

**Remark 3.1.** Note that for wave functions $\psi_j$ with $\|\psi_j\|=1$, one has

$$\|\psi_i-\psi_j\|^2 = 2\mathrm{Re}(1-h_{ij}) \le 2|1-h_{ij}|, \quad h_{ij} := \langle\psi_i,\psi_j\rangle.$$

Thus, defining relations can be paraphrased in terms of $h_{ij}$:

$$\begin{aligned}&\text{Complete synchronization} \iff \lim_{t\to\infty}\max_{i,j}|1-h_{ij}(t)| = 0.\\ &\text{Practical synchronization} \iff \lim_{\kappa\to+\infty}\sup_{0\le t\le T}\max_{i,j}|1-h_{ij}(t)| = 0.\end{aligned}$$

Before we present the synchronization estimates, we show that (1.2) admits a global unique solution. For global well-posedness, we introduce the energy space associated with (1.2):

$$X_H := \left\{u \in H^1(\mathbb{R}^d)\ :\ x\mapsto |x|u(x) \in L^2(\mathbb{R}^d)\right\}.$$

**Theorem 3.1.** *Suppose that*

$$1\le d\le 3, \quad \beta_{jk}>0, \quad \psi_j^0 \in X_H, \quad \text{for all } j,k = 1,\dots,N.$$

*Then, (1.2) has a global unique solution: for any $T>0$,*

$$\psi_j \in C([0,T];X_H)\cap L^\infty([0,T];H^1(\mathbb{R}^d))\cap L^{\frac{8}{d}}([0,T];L^4(\mathbb{R}^d)), \quad j=1,\dots,N.$$

**Proof.** We provide its proof in Appendix A. $\square$

### 3.1. Two-component GPL system

In this section, we present synchronization estimate for the GPL system under the same harmonic external potential. For simplicity, we set

$$d=1,\quad N=2,\quad V(x)=\frac{\omega^2}{2}x^2,\quad x\in\mathbb{R},\quad \omega>0,\quad \mathcal{A}=J_2,\quad h(t):=\langle\psi_1,\psi_2\rangle(t),\quad t\ge 0.$$

Under this setting, system (1.2) becomes

$$\begin{cases} \mathrm{i}\partial_t\psi_1 = -\frac{1}{2}\partial_{xx}\psi_1 + \frac{1}{2}\omega^2x^2\psi_1 + \beta_{11}|\psi_1|^2\psi_1 + \beta_{12}|\psi_2|^2\psi_1 + \frac{\mathrm{i}\kappa}{4}\left(\psi_2 - h(t)\psi_1\right), \\ \mathrm{i}\partial_t\psi_2 = -\frac{1}{2}\partial_{xx}\psi_2 + \frac{1}{2}\omega^2x^2\psi_2 + \beta_{21}|\psi_1|^2\psi_2 + \beta_{22}|\psi_2|^2\psi_2 + \frac{\mathrm{i}\kappa}{4}\left(\psi_1 - \bar{h}(t)\psi_2\right), \\ (\psi_1,\psi_2)(x,0) = (\psi_1^0(x),\psi_2^0(x)), \quad (x,t)\in\mathbb{R}\times\mathbb{R}_+, \quad \|\psi_1^0\| = \|\psi_2^0\| = 1. \end{cases} \tag{3.1}$$

For a solution $(\psi_1, \psi_2)$ to (3.1), we define several dynamic quantities:

$$
\begin{aligned}
& x_c^j(t) := \int_{\mathbb{R}} x|\psi_j(x,t)|^2 dx, \quad x_c(t) := x_c^1(t) + x_c^2(t), \quad j = 1, 2, \quad t \ge 0, \\
& P_c^j(t) := \int_{\mathbb{R}} \mathrm{Im}\left(\bar{\psi}_j(x,t)\nabla\psi_j(x,t)\right) dx, \quad P_c(t) := P_c^1(t) + P_c^2(t), \\
& \psi_d(x,t) := \psi_1(x,t) - \psi_2(x,t), \quad (x,t) \in \mathbb{R} \times \mathbb{R}_+, \\
& x_d(t) := \int_{\mathbb{R}} x|\psi_d(x,t)|^2 dx, \quad P_d(t) := \int_{\mathbb{R}} \mathrm{Im}(\bar{\psi}_d(x,t)\nabla\psi_d(x,t))dx.
\end{aligned}
\tag{3.2}
$$

Next, we state our first main result of this section without the proof.

**Theorem 3.2.** *Suppose that the system parameters and the initial data satisfy*

$$
\mathcal{B} = \beta J_2, \quad \langle \psi_1^0, \psi_2^0 \rangle \neq -1, \tag{3.3}
$$

*and let $(\psi_1, \psi_2)$ be a global solution to (3.1). Then, the following assertions hold.*

(1) *The complete synchronization emerges:*

$$
\lim_{t\to\infty} \|\psi_1(t) - \psi_2(t)\| = 0.
$$

(2) *The center-of-mass $x_c$ approaches to the periodic harmonic motion asymptotically: there exist positive constants $\alpha_1$ and $\alpha_2$ such that*

$$
\lim_{t\to\infty} |x_c(t) - (\alpha_1 \cos\omega t + \alpha_2 \sin\omega t)| = 0.
$$

**Proof.** (i) Note that the relation $(3.1)_1 \times \bar{\psi}_2 - \overline{(3.1)_2} \times \psi_1$ yields

$$
\dot{h} = \frac{\kappa}{2}(1 - h^2), \quad t > 0. \tag{3.4}
$$

Then, (3.4) can be solved as

$$
h(t) = \frac{(1+h^0)e^{\kappa t} - (1-h^0)}{(1-h^0) + (1+h^0)e^{\kappa t}}, \quad t > 0, \quad h(0) = h^0. \tag{3.5}
$$

Hence, since the initial data satisfy $h^0 \neq -1$, it follows from the explicit formula (3.5) that

$$
\lim_{t\to\infty} h(t) = 1.
$$

(ii) The second assertion will be proved in the following two steps:

- (Step A): First, we derive the dynamics of $(x_c, P_c)$ and $(x_d, P_d)$ introduced in (3.2).
- (Step B): We use preparatory lemmas and the assumption (3.3) to study the dynamics of $(x_c, P_c, x_d, P_d)$.

We leave the rigorous justification of the steps above in Section 4. □

### *3.2. Multi-component GPL system*

Below, we begin with several notation.

(1) For the network structure $\mathcal{A} = (a_{jk})$, we define the minimum average and the maximal difference:

$$
\|\mathcal{A}\|_\infty := \max_{j,k} |a_{jk}|, \qquad d_j^{\mathrm{av}}(\mathcal{A}) := \frac{1}{N}\sum_{k=1}^N a_{jk}, \qquad \delta(\mathcal{A}) := \max_k\Big(\max_{j,l} |a_{jk} - a_{lk}|\Big).
$$

(2) For the interaction matrix $\mathcal{B} = (\beta_{ij})$ which is a perturbation of a constant matrix $\beta J_N$, we set

$$
R(\mathcal{B}) := \max_{i\neq j} |\beta_{ij} - \beta|, \qquad \delta(\mathcal{B}) := \max_k\Big(\max_{j,l} |\beta_{jk} - \beta_{lk}|\Big).
$$

(3) For the external one-body potential $\{V_j\}$, we introduce a distance in $L^\infty$-norm:

$$
D(V) := \max_{i,j} \|V_i - V_j\|_\infty.
$$

In what follows, we present our main results according to the type of interaction matrix $\mathcal{B} = (\beta_{ij})$. As mentioned in Remark 3.1, it suffices to estimate the terms $1 - h_{ij}$. Our second main result corresponds to

$$
\mathcal{B} = \beta J_N, \quad \beta > 0.
$$

In this case, we expect that the complete synchronization can occur. For this, we define the synchronization functional as the maximum of $1 - h_{ij}$:

$$
\mathcal{S}(H(t)) := \max_{i,j} |1 - h_{ij}(t)|, \quad t \ge 0
$$

Then, since $\mathcal{S}(H)$ is Lipschitz continuous, it is differentiable almost everywhere. For notational simplicity, we set

$$\lambda(\mathcal{A}) := \min_j d_j^{\mathrm{av}}(\mathcal{A}) - \delta(\mathcal{A}).$$

**Theorem 3.3** (*Fully Identical Interactions*). *Suppose that system parameters, interaction matrix, network topology and the initial data satisfy*

$$\kappa > 0, \quad D(V) = 0, \quad \mathcal{B} = \beta J_N, \quad \lambda(\mathcal{A}) > 0, \quad \mathcal{S}(H^0) < \frac{\lambda(\mathcal{A})}{\|\mathcal{A}\|_\infty}, \tag{3.6}$$

*and let $\psi_j$ be a global smooth solution to (2.3) with $\|\psi_j^0\| = 1$. Then, we have the complete synchronization with exponential decay rate:*

$$\mathcal{S}(H(t)) \le \mathcal{O}(1) e^{-\kappa\lambda(\mathcal{A})t}, \quad t \ge 0.$$

**Proof.** We postpone its detailed proof in Section 5.1. □

**Remark 3.2.** Note that we do not require all $a_{jk}$ to be positive unlike the setting in [43] for the Schrödinger–Lohe system. In fact, some of $a_{jk}$ can take negative values. For instance, the following network topology is admissible:

$$\mathcal{A} = \begin{pmatrix} 1 & 1 & \cdots & 1 & -1 \\ 1 & 1 & \cdots & 1 & -1 \\ \vdots & \vdots & \ddots & \vdots & \vdots \\ 1 & 1 & \cdots & 1 & -1 \end{pmatrix}.$$

Then, for $\mathcal{A}$, we have

$$d_i^{\mathrm{av}}(\mathcal{A}) = \frac{N-2}{N} = 1 - \frac{2}{N}, \quad \text{for } i = 1, \dots, N \quad \text{and} \quad \delta(\mathcal{A}) = 0.$$

One can check that this network structure fits in our setting $(3.6)_4$:

$$\lambda(\mathcal{A}) = \min_j d_j^{\mathrm{av}}(\mathcal{A}) - \delta(A) = 1 - \frac{2}{N} > 0.$$

Next, we move on to the weakly interacting case:

$$\mathcal{B} = \beta J_N + \mathrm{diag}(\varepsilon_1, \dots, \varepsilon_N) : \quad \text{which is a perturbation of a constant matrix } \beta J_N.$$

In this case, we derive the practical synchronization estimate. For notational simplicity, we set

$$\Sigma := (\varepsilon_1, \dots, \varepsilon_N), \qquad D(\Sigma) := \max_{i,j} |\varepsilon_i - \varepsilon_j|, \qquad \|\Sigma\|_\infty := \max_i |\varepsilon_i|.$$

**Theorem 3.4** (*Weakly Identical Interactions*). *Suppose that system parameters, interaction matrix, network topology and the initial data satisfy*

$$\begin{aligned} & T \in (0, \infty), \quad \kappa > 0, \quad \lambda(\mathcal{A}) > 0, \quad D(V) < D(\Sigma), \quad \|\Sigma\|_\infty < \frac{|\lambda(\mathcal{A})|^2}{16\|\mathcal{A}\|_\infty(1 + M(T)^2)}\kappa, \\ & \mathcal{S}(H^0) < \frac{\kappa\lambda(\mathcal{A}) + \sqrt{\big(\kappa\lambda(\mathcal{A})\big)^2 - 8\kappa\|\mathcal{A}\|_\infty\|\Sigma\|_\infty\Big(2M(T)^3 + M(T)^2 + 1\Big)}}{2\kappa\|\mathcal{A}\|_\infty}, \end{aligned} \tag{3.7}$$

*and let $\psi_j$ be a global smooth solution to (2.3) satisfying a priori condition:*

$$\sup_{0 \le t \le T} \max_j \|\psi_j(t)\|_4 \le M(T) < \infty.$$

*Then, we have a practical synchronization on the finite interval $[0, T)$:*

$$\sup_{0 \le t \le T} \mathcal{S}(H(t)) \le \mathcal{O}(1) \left( \frac{\|\Sigma\|_\infty\Big(2M(T)^3 + M(T)^2 + 1\Big)}{\kappa\lambda(\mathcal{A})} \right). \tag{3.8}$$

**Proof.** The detailed proof will be given in Section 5.2. □

**Remark 3.3.** Note that the result of Theorem 3.4 does not depend on the value of $\beta$, and the estimate (3.8) yields practical synchronization estimate in Definition 3.1:

$$\lim_{\kappa \to \infty} \sup_{0 \le t \le T} \mathcal{S}(H(t)) = 0, \quad \text{for any} \quad T \in (0, \infty).$$

Finally, we consider the heterogeneous case:

$$\mathcal{B} = \begin{pmatrix} \beta & \beta_{12} & \cdots & \beta_{1N} \\ \beta_{21} & \beta & \cdots & \beta_{2N} \\ \vdots & \vdots & \ddots & \vdots \\ \beta_{N1} & \beta_{N2} & \cdots & \beta \end{pmatrix} + \mathrm{diag}(\varepsilon_1, \dots, \varepsilon_N).$$

For notational simplicity, we set

$$G := 2M(T)^4\big(R(\mathcal{B}) + \|\Sigma\|_\infty + \delta(\mathcal{B})\big) + D(V). \tag{3.9}$$

**Theorem 3.5** (*Heterogeneous Interactions*)**.** *Suppose that system parameters, interaction matrix, network topology and the initial data satisfy*

$$\lambda(\mathcal{A}) > 0, \quad \kappa > \frac{4G\|\Sigma\|_\infty}{(\lambda(\mathcal{A}))^2}, \quad \mathcal{S}(H^0) < \frac{\kappa\lambda(\mathcal{A}) + \sqrt{(\kappa\lambda(\mathcal{A}))^2 - 4\kappa G\|\Sigma\|_\infty}}{2\kappa\|\Sigma\|_\infty}, \tag{3.10}$$

*and let $\psi_j$ be a global smooth solution to (2.3) satisfying a priori condition:*

$$\sup_{0\le t\le T} \max_j \|\psi_j(t)\|_4 \le M(T) < \infty.$$

*Then, we have*

$$\sup_{0\le t\le T} \mathcal{S}(H(t)) \le \frac{2G}{\kappa\lambda(\mathcal{A})}.$$

**Proof.** We present its proof in Section 5.3. □

## 4. A two-component GPL system

In this section, we provide a proof of Theorem 3.2. For this, we provide dynamics of quantities introduced in (3.2).

### 4.1. Preparatory lemmas

Below, we provide three lemmas to be used in the proof of Theorem 3.2. First, we set $R(t)$ to be a real part of $h(t) := \langle \psi_1(t), \psi_2(t)\rangle$:

$$R(t) := \mathrm{Re}h(t), \quad t \ge 0.$$

**Lemma 4.1.** *Let $(\psi_1, \psi_2)$ be a global smooth solution to (3.1). Then, $(x_c, P_c)$ defined in (3.2) satisfies the following dynamics:*

$$\begin{cases} \dot{x}_c = \dfrac{\kappa}{2}(1-R)x_c + P_c - \dfrac{\kappa}{2}x_d, \quad t > 0, \\ \dot{P}_c = -\omega^2 x_c + \dfrac{\kappa}{2}(1-R)P_c - \dfrac{\kappa}{2}P_d. \end{cases} \tag{4.1}$$

**Proof.** • Derivation of dynamics of $x_c$: We use the identity (2.4) and defining relations (3.2) to see

$$\begin{aligned} \dot{x}_c &= \frac{d}{dt}\int_{\mathbb{R}} \Big(x|\psi_1|^2 + x|\psi_2|^2\Big)dx = 2\int_{\mathbb{R}} x\Big[\mathrm{Re}(\partial_t\bar{\psi}_1 \cdot \psi_1) + x\mathrm{Re}(\partial_t\bar{\psi}_2 \cdot \psi_2)\Big]dx \\ &= 2\int_{\mathbb{R}} x\mathrm{Re}\left[-\frac{\mathrm{i}}{2}\Delta\bar{\psi}_1\psi_1 + \frac{\mathrm{i}}{2}\omega^2x^2|\psi_1|^2 + \mathrm{i}\beta_{11}|\psi_1|^4 + \mathrm{i}\beta_{12}|\psi_2|^2|\psi_1|^2\right]dx \\ &\quad + 2\int_{\mathbb{R}} x\mathrm{Re}\left[-\frac{\mathrm{i}}{2}\Delta\bar{\psi}_2\psi_2 + \frac{\mathrm{i}}{2}\omega^2x^2|\psi_2|^2 + \mathrm{i}\beta_{21}|\psi_1|^2|\psi_2|^2 + \mathrm{i}\beta_{22}|\psi_2|^4\right]dx \\ &\quad + \frac{\kappa}{2}\left(\int_{\mathbb{R}} x\mathrm{Re}\left(\psi_1\bar{\psi}_2 - \bar{h}|\psi_1|^2\right) + x\mathrm{Re}(\bar{\psi}_1\psi_2 - h|\psi_2|^2)dx\right) \\ &=: \mathcal{I}_{31} + \mathcal{I}_{32} + \mathcal{I}_{33}. \end{aligned} \tag{4.2}$$

Below, we consider $\mathcal{I}_{3k}$, $k = 1, 2, 3$, separately.
◇ (Estimate of $\mathcal{I}_{31}$): Since $\omega$, $\beta_{11}$ and $\beta_{12}$ are real, we see

$$\begin{aligned} \mathcal{I}_{31} &= 2\int_{\mathbb{R}} x\mathrm{Re}\left[-\frac{\mathrm{i}}{2}\Delta\bar{\psi}_1\psi_1 + \frac{\mathrm{i}}{2}\omega^2x^2|\psi_1|^2 + \mathrm{i}\beta_{11}|\psi_1|^4 + \mathrm{i}\beta_{12}|\psi_2|^2|\psi_1|^2\right]dx \\ &= \int_{\mathbb{R}} \mathrm{Re}(-\mathrm{i}x\Delta\psi_1\psi_1)\,dx = \int_{\mathbb{R}} \mathrm{Re}(\mathrm{i}\nabla(x\psi_1)\cdot\nabla\bar{\psi}_1)\,dx = \int_{\mathbb{R}} \mathrm{Re}(\mathrm{i}\psi_1\nabla\bar{\psi}_1) \\ &= \int_{\mathbb{R}} \mathrm{Im}(\bar{\psi}_1\nabla\psi_1)\,dx = P_c^1. \end{aligned} \tag{4.3}$$

$\diamond$ (Estimate of $\mathcal{I}_{32}$): Similarly, since $\beta_{21}$ and $\beta_{22}$ are also real, we have

$$\mathcal{I}_{32} = \int_{\mathbb{R}} \mathrm{Im}(\bar{\psi}_2 \nabla \psi_2)\, dx = P_c^2. \tag{4.4}$$

$\diamond$ (Estimate of $\mathcal{I}_{33}$) Recall the identity (2.8) to see

$$2\mathrm{Re}(\bar{\psi}_1\psi_2) = |\psi_1|^2 + |\psi_2|^2 - |\psi_1 - \psi_2|^2.$$

Hence, we find

$$\begin{aligned}
&\frac{\kappa}{2}\left(\int_{\mathbb{R}} x\mathrm{Re}\left(\psi_1\bar{\psi}_2 - \bar{h}|\psi_1|^2\right) + x\mathrm{Re}(\bar{\psi}_1\psi_2 - h|\psi_2|^2)dx\right) \\
&\qquad = \kappa \int_{\mathbb{R}} x\mathrm{Re}(\psi_1\bar{\psi}_2)\, dx - \frac{\kappa R}{2}\left(\int_{\mathbb{R}} x|\psi_1|^2 + x|\psi_2|^2\, dx\right) \\
&\qquad = \frac{\kappa}{2}\int_{\mathbb{R}} \left(x|\psi_1|^2 + x|\psi_2|^2 - x|\psi_1 - \psi_2|^2\right) dx - \frac{\kappa R}{2} x_c \\
&\qquad = \frac{\kappa}{2}x_c - \frac{\kappa}{2}x_d - \frac{\kappa R}{2}x_c.
\end{aligned} \tag{4.5}$$

In (4.2), we combine the estimates (4.3)–(4.5) to obtain the desired equation $(4.1)_1$:

$$\dot{x}_c = \frac{\kappa}{2}(1-R)x_c + P_c - \frac{\kappa}{2}x_d.$$

• Derivation of dynamics of $P_c$: We again use the defining relations (3.2) to get

$$\begin{aligned}
\dot{P}_c^1 &= \frac{d}{dt}\int_{\mathbb{R}} \mathrm{Im}(\bar{\psi}_1\nabla\psi_1)\, dx = \int_{\mathbb{R}} \mathrm{Im}(\partial_t\bar{\psi}_1\nabla\psi_1 + \bar{\psi}_1\partial_t\nabla\psi_1)\, dx \\
&= \int_{\mathbb{R}} \mathrm{Im}\left[\left(-\frac{\mathrm{i}}{2}\Delta\bar{\psi}_1 + \frac{\mathrm{i}}{2}\omega^2x^2\bar{\psi}_1 + \mathrm{i}\beta_{11}|\psi_1|^2\bar{\psi}_1 + \mathrm{i}\beta_{12}|\psi_2|^2\bar{\psi}_1\right)\nabla\psi_1\right] dx \\
&\quad + \int_{\mathbb{R}} \mathrm{Im}\left[\left(-\frac{\mathrm{i}}{2}\nabla\Delta\psi_1 + \mathrm{i}\nabla\left(\frac{\omega^2}{2}x^2\psi_1\right) + \mathrm{i}\beta_{11}\nabla(|\psi_1|^2\psi_1) + \mathrm{i}\beta_{12}\nabla(|\psi_2|^2\psi_1)\right)\bar{\psi}_1\right] \\
&\quad + \frac{\kappa}{4}\int_{\mathbb{R}} \mathrm{Im}\Big(\bar{\psi}_2\nabla\psi_1 - \bar{h}\bar{\psi}_1\nabla\psi_1 + \bar{\psi}_1\nabla\psi_2 - h\bar{\psi}_1\nabla\psi_1 \\
&\qquad\qquad + \bar{\psi}_1\nabla\psi_2 - \bar{h}\bar{\psi}_2\nabla\psi_2 + \bar{\psi}_2\nabla\psi_1 - h\bar{\psi}_2\nabla\psi_2\Big)dx \\
&= \int_{\mathbb{R}} \mathrm{Im}\left(-\frac{\mathrm{i}}{2}\Delta\bar{\psi}_1\nabla\psi_1 - \frac{\mathrm{i}}{2}\Delta\nabla\psi_1\bar{\psi}_1\right) dx + \int_{\mathbb{R}} \mathrm{Im}\left(\frac{\mathrm{i}}{2}\omega^2x^2\bar{\psi}_1\nabla\psi_1 + \mathrm{i}\nabla\left(\frac{\omega^2}{2}x^2\psi_1\right)\bar{\psi}_1\right) dx \\
&\quad + \int_{\mathbb{R}} \mathrm{Im}\Big(\mathrm{i}\beta_{11}|\psi_1|^2\bar{\psi}_1\nabla\psi_1 + \mathrm{i}\beta_{11}\nabla(|\psi_1|^2\psi_1)\bar{\psi}_1\Big) \\
&\quad + \int_{\mathbb{R}} \mathrm{Im}\Big(\mathrm{i}\beta_{12}|\psi_2|^2\bar{\psi}_1\nabla\psi_1 + \mathrm{i}\beta_{12}\nabla(|\psi_2|^2\psi_1)\bar{\psi}_1\Big) \\
&\quad + \frac{\kappa}{4}\int_{\mathbb{R}} \mathrm{Im}\Big(\bar{\psi}_2\nabla\psi_1 - \bar{h}\bar{\psi}_1\nabla\psi_1 + \bar{\psi}_1\nabla\psi_2 - h\bar{\psi}_1\nabla\psi_1\Big)\, dx \\
&=: \mathcal{I}_{41} + \mathcal{I}_{42} + \mathcal{I}_{43} + \mathcal{I}_{44} + \mathcal{I}_{45}.
\end{aligned}$$

Below, we provide the estimates of $\mathcal{I}_{4k},\ k = 1, \dots, 5$, respectively.

$\diamond$ (Estimate of $\mathcal{I}_{41}$): By direct calculation,

$$\begin{aligned}
\mathcal{I}_{41} &= \int_{\mathbb{R}} \mathrm{Im}\left(-\frac{\mathrm{i}}{2}\Delta\bar{\psi}_1\nabla\psi_1 - \frac{\mathrm{i}}{2}\nabla\Delta\psi_1\bar{\psi}_1\right) dx = \int_{\mathbb{R}} \mathrm{Im}\left(-\frac{\mathrm{i}}{2}\Delta\bar{\psi}_1\nabla\psi_1 + \frac{\mathrm{i}}{2}\Delta\psi_1\nabla\bar{\psi}_1\right) dx \\
&= 0,
\end{aligned}$$

where we used the fact that the second term is the complex conjugate of the first term.

$\diamond$ (Estimate of $\mathcal{I}_{42}$): Note that one has

$$\begin{aligned}
\mathcal{I}_{42} &= \int_{\mathbb{R}} \mathrm{Im}\left(\frac{\mathrm{i}}{2}\omega^2x^2\bar{\psi}_1\nabla\psi_1 + \mathrm{i}\nabla\left(\frac{\omega^2}{2}x^2\psi_1\right)\bar{\psi}_1\right) dx \\
&= \int_{\mathbb{R}} \mathrm{Im}\left(\frac{\mathrm{i}}{2}\omega^2x^2\bar{\psi}_1\nabla\psi_1 + \mathrm{i}\omega x|\psi_1|^2 + \frac{\mathrm{i}}{2}\omega^2x^2\nabla\psi_1\bar{\psi}_1\right) dx \\
&= -\omega^2\int_{\mathbb{R}} x|\psi_1|^2 = -\omega^2x_c^1.
\end{aligned}$$

◇ (Estimate of $\mathcal{I}_{43}+\mathcal{I}_{44}$): From straightforward calculation,

$$\begin{aligned}\mathcal{I}_{43}+\mathcal{I}_{44} &= \int_{\mathbb{R}} \mathrm{Im}\Big(\mathrm{i}\beta_{11}|\psi_1|^2\bar{\psi}_1\nabla\psi_1 + \mathrm{i}\beta_{11}\nabla(|\psi_1|^2\psi_1)\bar{\psi}_1\Big) \\ &\quad + \int_{\mathbb{R}} \mathrm{Im}\Big(\mathrm{i}\beta_{12}|\psi_2|^2\bar{\psi}_1\nabla\psi_1 + \mathrm{i}\beta_{12}\nabla(|\psi_2|^2\psi_1)\bar{\psi}_1\Big) \\ &= \int_{\mathbb{R}} \mathrm{Im}\Big(\mathrm{i}\beta_{11}\nabla(|\psi_1|^4) + \mathrm{i}\beta_{12}\nabla(|\psi_1|^2|\psi_2|^2)\Big) = 0.\end{aligned}$$

◇ (Estimate of $\mathcal{I}_{45}$): Note that the following identity holds:

$$\bar{\psi}_2\nabla\psi_1 + \bar{\psi}_1\nabla\psi_2 = \bar{\psi}_1\nabla\psi_1 + \bar{\psi}_2\nabla\psi_2 - \bar{\psi}_d\nabla\psi_d.$$

Then, we have

$$\begin{aligned}\mathcal{I}_{45} &= \frac{\kappa}{4}\int_{\mathbb{R}} \mathrm{Im}\Big(\bar{\psi}_2\nabla\psi_1 - \bar{h}\bar{\psi}_1\nabla\psi_1 + \bar{\psi}_1\nabla\psi_2 - h\bar{\psi}_1\nabla\psi_1\Big)\,dx \\ &= -\frac{\kappa}{4}(\bar{h}+h)P_c^1 + \frac{\kappa}{4}\int_{\mathbb{R}} \mathrm{Im}\Big(\bar{\psi}_2\nabla\psi_1 + \bar{\psi}_1\nabla\psi_2\Big)\,dx \\ &= -\frac{\kappa}{2}RP_c^1 + \frac{\kappa}{4}(P_c - P_d).\end{aligned}$$

Hence, we combine all estimates to find

$$\dot{P}_c^1 = \omega^2 x_c^1 - \frac{\kappa}{2}RP_c^1 + \frac{\kappa}{4}(P_c - P_d). \tag{4.6}$$

Similarly, we have

$$\dot{P}_c^2 = \omega^2 x_c^2 - \frac{\kappa}{2}RP_c^2 + \frac{\kappa}{4}(P_c - P_d). \tag{4.7}$$

Finally, we add (4.6) and (4.7) to yield the desired equation $(4.1)_2$.

$$\dot{P}_c = -\omega^2 x_c - \frac{\kappa}{2}RP_c + \frac{\kappa}{2}(P_c - P_d) = -\omega^2 x_c + \frac{\kappa}{2}(1-R)P_c - \frac{\kappa}{2}P_d. \quad \square$$

**Remark 4.1.** 1. If $\kappa = 0$, (4.1) reduces to the harmonic oscillator case:

$$\dot{x}_c = P_c, \quad \dot{P}_c = -\omega^2 x_c; \quad \text{or equivalently} \quad \ddot{x}_c + \omega^2 x_c = 0. \tag{4.8}$$

Then, (4.8) can be explicitly solved as

$$x_c(t) = x_c(0)\cos\omega t + \frac{\dot{x}_c(0)}{\omega}\sin\omega t, \quad t \geq 0,$$

which is a periodic harmonic motion with a period $\omega$.

*2.* Note that system (4.1) does not depend on the choice of $\beta_{ij}$ and is not closed, as it contains $(x_d, P_d)$. To close the hierarchy, we consider the identical case:

$$\beta_{11} = \beta_{12} = \beta_{21} = \beta_{22} =: \beta \quad \text{or} \quad \mathcal{B} = \beta J_2, \tag{4.9}$$

and derive the dynamics for $(x_d, P_d)$ in the following lemma.

**Lemma 4.2.** *Let $(\psi_1, \psi_2)$ be a global smooth solution to (3.1) with $\mathcal{B} = \beta J_2$. Then, $(x_d, P_d)$ satisfies the following dynamics:*

$$\begin{cases}\dot{x}_d = -\frac{\kappa}{2}(1+R)x_d + P_d, \quad t > 0, \\ \dot{P}_d = -\omega^2 x_d - \frac{\kappa}{2}(1+R)P_d.\end{cases}$$

**Proof.** First, note that $\psi_d$ satisfies

$$\mathrm{i}\partial_t\psi_d = -\frac{1}{2}\Delta\psi_d + \frac{\omega^2}{2}x^2\psi_d + \beta(|\psi_1|^2 + |\psi_2|^2)\psi_d + \frac{\mathrm{i}\kappa}{4}\Big((1+\bar{h})\psi_2 - (1+h)\psi_1\Big). \tag{4.10}$$

• Derivation of dynamics of $x_d$: We use (2.4) and (4.10) to get

$$\begin{aligned}\dot{x}_d &= \frac{d}{dt}\int_{\mathbb{R}} x|\psi_d|^2 dx = 2\int_{\mathbb{R}} x\mathrm{Re}(\partial_t\bar{\psi}_d\cdot\psi_d)dx \\ &= P_d + \frac{\kappa}{2}\int_{\mathbb{R}} x\mathrm{Re}\Big(-(1+h)|\psi_2|^2 - (1+\bar{h})|\psi_1|^2 + (1+\bar{h})\bar{\psi}_1\psi_2 + (1+h)\bar{\psi}_2\psi_1\Big)dx \\ &= P_d - \frac{\kappa}{2}(1+R)x_c + \frac{\kappa}{2}(1+R)(x_c - x_d) \\ &= P_d - \frac{\kappa}{2}(1+R)x_d.\end{aligned}$$

• Derivation of dynamics of $P_d$: Similar to the estimate of $x_d$, we have

$$\begin{aligned}\dot{P}_d &= \int_{\mathbb{R}} \mathrm{Im}\Big(\partial_t\bar{\psi}_d \nabla\psi_d + \bar{\psi}_d\partial_t\nabla\psi_d\Big)dx \\ &= -\omega^2 x_d + \frac{\kappa}{4}\int_{\mathbb{R}} \mathrm{Im}\Big((1+h)\bar{\psi}_2 - (1+\bar{h})\bar{\psi}_1\Big)(\nabla\psi_1 - \nabla\psi_2) \\ &\qquad\qquad + \mathrm{Im}(\bar{\psi}_1 - \bar{\psi}_2)\Big((1+\bar{h})\nabla\psi_2 - (1+h)\nabla\psi_1\Big)dx \\ &= -\omega^2 x_d - \frac{\kappa}{2}(1+R)P_c + \frac{\kappa}{2}(1+R)(P_c - P_d) \\ &= -\omega^2 x_d - \frac{\kappa}{2}(1+R)P_d. \quad \square\end{aligned}$$

Next, we provide an explicit solution formula for the following two-dimensional system:

$$\begin{cases}\dot{x} = f(t)x + py + g_1(t), \quad t > 0, \\ \dot{y} = -qx + f(t)y + g_2(t), \\ (x,y)(0) = (x^0, y^0).\end{cases} \tag{4.11}$$

To rewrite (4.11) in a compact form, we set

$$Z(t) := \begin{pmatrix} x(t) \\ y(t)\end{pmatrix}, \quad A(t) := \begin{pmatrix} f(t) & p \\ -q & f(t)\end{pmatrix}, \quad G(t) := \begin{pmatrix} g_1(t) \\ g_2(t)\end{pmatrix}.$$

Then, (4.11) can be rewritten as a matrix form:

$$\begin{cases}\dot{Z}(t) = A(t)Z(t) + G(t), \quad t > 0, \\ Z(0) = (x^0, y^0).\end{cases} \tag{4.12}$$

**Lemma 4.3.** *Suppose that $p$ and $q$ are positive constants and $f : \mathbb{R}_+ \to \mathbb{R}_+$ is a continuous time-dependent function. Then, the solution $(x(t), y(t))$ is given by the following explicit formula:*

$$\begin{aligned}\begin{pmatrix} x(t) \\ y(t)\end{pmatrix} &= \begin{pmatrix} e^{\int_0^t f(s)ds} & 0 \\ 0 & e^{\int_0^t f(s)ds}\end{pmatrix}\begin{pmatrix} \cos(\sqrt{pq}t) & \sqrt{\frac{p}{q}}\sin(\sqrt{pq}t) \\ -\sqrt{\frac{q}{p}}\sin(\sqrt{pq}t) & \cos(\sqrt{pq}t)\end{pmatrix}\begin{pmatrix} x^0 \\ y^0\end{pmatrix} \\ &\quad + e^{\int_0^t A(s)ds}\int_0^t e^{-\int_0^s A(\tau)d\tau}G(s)ds, \quad t \geq 0.\end{aligned}$$

**Proof.** Since the proof is lengthy, we postpone its proof in Appendix B. $\square$

*4.2. Proof of Theorem 3.2*

Now, we are ready to provide the proof of Theorem 3.2 in two steps.

• Step A (Derivation of explicit formula for $(x_d, P_d)$): Consider the dynamical system for $(x_d, P_d)$:

$$\begin{cases}\dot{x}_d = -\frac{\kappa}{2}(1+R)x_d + P_d, \quad t > 0, \\ \dot{P}_d = -\omega^2 x_d - \frac{\kappa}{2}(1+R)P_d.\end{cases}$$

We set

$$f(t) = -\frac{\kappa}{2}(1+R(t)), \quad p = 1, \quad q = \omega^2, \quad G(t) = 0,$$

and apply Lemma 4.3 to derive a representation relation:

$$\begin{aligned}\begin{pmatrix} x_d(t) \\ P_d(t)\end{pmatrix} &= \begin{pmatrix} e^{-\frac{\kappa}{2}\int_0^t(1+R(s))ds} & 0 \\ 0 & e^{-\frac{\kappa}{2}\int_0^t(1+R(s))ds}\end{pmatrix}\begin{pmatrix} \cos(\omega t) & \frac{1}{\omega}\sin(\omega t) \\ -\omega\sin(\omega t) & \omega\cos(\omega t)\end{pmatrix}\begin{pmatrix} x_d^0 \\ P_d^0\end{pmatrix} \\ &= \begin{pmatrix} \cos(\omega t)e^{-\frac{\kappa}{2}\int_0^t(1+R(s))ds} & \frac{1}{\omega}\sin(\omega t)e^{-\frac{\kappa}{2}\int_0^t(1+R(s))ds} \\ -\omega\sin(\omega t)e^{-\frac{\kappa}{2}\int_0^t(1+R(s))ds} & \omega\cos(\omega t)e^{-\frac{\kappa}{2}\int_0^t(1+R(s))ds}\end{pmatrix}\begin{pmatrix} x_d^0 \\ P_d^0\end{pmatrix}.\end{aligned} \tag{4.13}$$

• Step B (Derivation of explicit formula for $(x_c, P_c)$): Together with the representation formula for $(x_d, P_d)$, we use Lemma 4.3 to derive representation explicit formula for (4.1). To do this, we write (4.1) into compact form:

$$\begin{cases}\dot{W}(t) = E(t)W(t) - \frac{\kappa}{2}Y(t), \quad t > 0, \\ W(0) = (x_c^0, P_c^0),\end{cases} \tag{4.14}$$

where $W, E$ and $Z$ are defined as follows:

$$W(t) := \begin{pmatrix} x_c(t) \\ P_c(t) \end{pmatrix}, \quad E(t) := \begin{pmatrix} \frac{\kappa}{2}(1-R(t)) & 1 \\ -\omega^2 & \frac{\kappa}{2}(1-R(t)) \end{pmatrix}, \quad Y(t) := \begin{pmatrix} x_d(t) \\ P_d(t) \end{pmatrix}.$$

Since (4.14) has the same form of (4.12), it follows from Lemma 4.3 that

$$W(t) = W(0)e^{\int_0^t E(s)ds} - \frac{\kappa}{2}e^{-\int_0^t E(s)ds}\int_0^t e^{\int_0^s E(\tau)d\tau}Y(s)ds.$$

Following the argument in Lemma 4.3, we calculate $e^{\int_0^t E(s)ds}$ as follows:

$$e^{\int_0^t E(s)ds} = \begin{pmatrix} e^{\frac{\kappa}{2}\int_0^t(1-R(s))ds} & 0 \\ 0 & e^{\frac{\kappa}{2}\int_0^t(1-R(s))ds} \end{pmatrix}\begin{pmatrix} \cos(\omega t) & \sin(\omega t) \\ -\omega\sin(\omega t) & \omega\cos(\omega t) \end{pmatrix}.$$

We again apply Lemma 4.3 to obtain

$$\begin{aligned}
\begin{pmatrix} x_c(t) \\ P_c(t) \end{pmatrix} &= e^{\int_0^t E(s)ds}W_0 + e^{\int_0^t E(s)ds}\begin{pmatrix} \frac{x_d^0}{\kappa}\left(1-e^{-\kappa t}\right) \\ \frac{P_d^0}{\kappa}\left(1-e^{-\kappa t}\right) \end{pmatrix} \\
&= \begin{pmatrix} \cos(\omega t)e^{\frac{\kappa}{2}\int_0^t(1-R(s))ds} & \sin(\omega t)e^{\frac{\kappa}{2}\int_0^t(1-R(s))ds} \\ -\omega\sin(\omega t)e^{\frac{\kappa}{2}\int_0^t(1-R(s))ds} & \omega\cos(\omega t)e^{\frac{\kappa}{2}\int_0^t(1-R(s))ds} \end{pmatrix}\begin{pmatrix} x_c^0 + \frac{x_d^0}{\kappa}(1-e^{-\kappa t}) \\ P_c^0 + \frac{P_d^0}{\kappa}(1-e^{-\kappa t}) \end{pmatrix}.
\end{aligned}$$

On the other hand, it follows from the explicit formula (3.5) that $1-R(t)$ converges to zero with exponential rate:

$$\begin{aligned}
1-R(t) = \mathrm{Re}(1-h(t)) &= \frac{2|1-h^0|^2 + 2(1-|h^0|^2)e^{\kappa t}}{|1-h^0|^2 + 2(1-|h^0|^2)e^{\kappa t} + |1+h^0|^2e^{2\kappa t}}, \\
&\le \frac{2|1-h^0|^2}{|1+h^0|^2}e^{-2\kappa t} + \frac{2(1-|h^0|^2)}{|1+h^0|^2}e^{-\kappa t}.
\end{aligned}$$

Hence, if we set

$$\mathcal{J}(t) := \exp\left(\frac{\kappa}{2}\int_0^t\left(1-R(s)\right)ds\right), \quad t \ge 0.$$

then the limit of $\mathcal{J}(t)$ exists:

$$\mathcal{J}_\infty := \lim_{t\to\infty}\mathcal{J}(t).$$

Now, we write an explicit formula for $x_c(t)$:

$$x_c(t) = \left(x_c^0 + \frac{x_d^0}{\kappa}(1-e^{-\kappa t})\right)\mathcal{J}(t)\cos(\omega t) + \left(P_c^0 + \frac{P_d^0}{\kappa}(1-e^{-\kappa t})\right)\mathcal{J}(t)\sin(\omega t). \tag{4.15}$$

Therefore, we can conclude that there exist positive constants $\alpha_1$ and $\alpha_2$ depending on initial data and system parameters such that

$$\lim_{t\to\infty}\left|x_c(t) - \left(\alpha_1\cos(\omega t) + \alpha_2\sin(\omega t)\right)\right| = 0,$$

where $\alpha_1$ and $\alpha_2$ are defined as

$$\alpha_1 := x_c^0 + \frac{x_d^0}{\kappa}\mathcal{J}_\infty, \quad \alpha_2 := P_c^0 + \frac{P_d^0}{\kappa}\mathcal{J}_\infty.$$

This completes the proof of the second assertion in Theorem 3.2.

**Remark 4.2.** 1. Suppose that $h^0 = \langle\psi_1^0, \psi_2^0\rangle \in \mathbb{R}$. Then, the explicit formula (3.5) yields

$$1-R(t) = \frac{2(1-h^0)}{(1-h^0)+(1+h^0)e^{\kappa t}}.$$

From straightforward calculation, we have

$$\int_0^\infty\left(1-R(t)\right)dt = \int_0^\infty\frac{2(1-h^0)}{(1-h^0)+(1+h^0)e^{\kappa t}}dt = \frac{2}{\kappa}\log\frac{2}{1+h^0}.$$

This yields

$$\mathcal{J}_\infty = \lim_{t\to\infty}\mathcal{J}(t) = \left(\frac{2}{1+h^0}\right)^{\frac{2}{\kappa}}.$$

In this case, we can find explicit values of $(\alpha_1, \alpha_2)$:

$$\alpha_1 = x_c^0 + \frac{x_d^0}{\kappa}\left(\frac{2}{1+R_0}\right)^{\frac{2}{\kappa}}, \quad \alpha_2 = P_c^0 + \frac{P_d^0}{\kappa}\left(\frac{2}{1+R_0}\right)^{\frac{2}{\kappa}}. \tag{4.16}$$

2. Consider the symmetric initial data such that

$$\psi_1^0 = \mathcal{M}(x - x_0), \quad \psi_2^0 = \mathcal{M}(x + x_0),$$

where $\mathcal{M}(z)$ is defined to be the Gaussian function with mean zero, i.e.,

$$\mathcal{M}(z) := \frac{1}{\sqrt{2\pi}} e^{-\frac{1}{2}z^2}, \quad z \in \mathbb{R}.$$

Then, we can easily check that

$$R^0 := \mathrm{Re}\langle \psi_1^0, \psi_2^0 \rangle, \quad x_c^0 = x_d^0 = P_c^0 = P_d^0 = 0.$$

Hence, it follows from our explicit formula (4.15) and (4.16) that

$$x_c(t) \equiv 0, \quad t > 0.$$

As a direct application of the previous results, we have the following corollary.

**Corollary 4.1.** *Let $(\psi_1, \psi_2)$ be a global smooth solution of (3.1) with initial data $(\psi_1^0, \psi_2^0)$ and condition (4.9). Then, the following assertions hold:*

$$\lim_{t\to\infty} x_d(t) = 0 \quad \textit{and} \quad \lim_{t\to\infty} \left| \int_{\mathbb{R}} x|\psi_1(x,t)|^2 dx - \int_{\mathbb{R}} x|\psi_2(x,t)|^2 dx \right| = 0. \tag{4.17}$$

**Proof.** (i) For the first assertion, the explicit formula (4.13) gives

$$x_d(t) = x_d^0 \cos(\omega t) e^{-\frac{\kappa}{2}\int_0^t (1+R(s))ds} + \frac{P_d^0}{\omega}\sin(\omega t) e^{-\frac{\kappa}{2}\int_0^t (1+R(s))ds}. \tag{4.18}$$

Our claim is that

$$\lim_{t\to\infty} e^{-\frac{\kappa}{2}\int_0^t (1+R(s))ds} = 0. \tag{4.19}$$

Since we know that $R(t)$ converges to 1, there exists a finite time $T_0$ such that

$$1 + R(t) > \frac{3}{2} \quad \text{for } t > T_0.$$

Hence, one has

$$e^{-\frac{\kappa}{2}\int_{T_0}^t (1+R(s))ds} < e^{-\frac{3}{2}(t-T_0)}, \quad t > T_0.$$

This shows our claim. In (4.18), we use (4.19) to establish the first assertion.
(ii) From the first assertion, we have

$$\lim_{t\to\infty} x_d(t) = 0 \quad \text{or equivalently} \quad \lim_{t\to\infty} \int_{\mathbb{R}} x|\psi_1(x,t) - \psi_2(x,t)|^2 dx = 0, \tag{4.20}$$

and (4.20) can be written as

$$\lim_{t\to\infty} \int_0^\infty x\Big(|\psi_1(x,t) - \psi_2(x,t)|^2 - |\psi_1(-x,t) - \psi_2(-x,t)|^2\Big) dx = 0,$$

where we used $\int_{-\infty}^\infty = \int_0^\infty + \int_{-\infty}^0$ and the change of variable in the second integral. Then, it follows from the positivity of integrand in the above relation that we have

$$\begin{aligned} &\int_0^\infty x|\psi_1(x,t) - \psi_2(x,t)|^2 dx \le x_d(t), \quad \int_0^\infty x|\psi_1(-x,t) - \psi_2(-x,t)|^2 dx \le x_d(t), \\ &\int_{\mathbb{R}} x\Big(|\psi_1(x,t)|^2 - |\psi_2(x,t)|^2\Big) dx \\ &\qquad = \int_0^\infty x\Big(|\psi_1(x,t)|^2 - |\psi_2(x,t)|^2\Big) + x\Big(|\psi_2(-x,t)|^2 - |\psi_1(-x,t)|^2\Big) dx. \end{aligned} \tag{4.21}$$

On the other hand, note that

$$\begin{aligned}
&\int_0^\infty x\Big(|\psi_1(x,t)|^2 - |\psi_2(x,t)|^2\Big)dx \\
&\quad = \int_0^\infty \sqrt{x}\big(|\psi_1(x,t)| - |\psi_2(x,t)|\big)\sqrt{x}\big(|\psi_1(x,t)| + |\psi_2(x,t)|\big)dx \\
&\quad \le \int_0^\infty \sqrt{x}|\psi_1(x,t) - \psi_2(x,t)|\sqrt{x}\Big||\psi_1(x,t)| + |\psi_2(x,t)|\Big|dx \\
&\quad \le \left(\int_0^\infty x|\psi_1(x,t) - \psi_2(x,t)|^2 dx\right)^{\frac{1}{2}} \left(\int_0^\infty 2x\Big(|\psi_1(x,t)|^2 + |\psi_2(x,t)|^2\Big)dx\right)^{\frac{1}{2}} \\
&\quad \le \sqrt{2x_d(t)x_c(t)},
\end{aligned} \tag{4.22}$$

where we used the following triangle inequality in the first inequality: for $u, v \in \mathbb{C}$,

$$\Big||u| - |v|\Big| \le |u - v|.$$

By the same argument, we also find

$$\int_0^\infty x\Big(|\psi_2(-x,t)|^2 - |\psi_1(-x,t)|^2\Big)dx \le \sqrt{2x_d(t)x_c(t)}. \tag{4.23}$$

We collect (4.21)–(4.23) to conclude that

$$\int_{\mathbb{R}} x\Big(|\psi_1(x,t)|^2 - |\psi_2(x,t)|^2\Big)dx \le 2\sqrt{2x_d(t)x_c(t)}.$$

Since $x_d(t)$ tends to zero and $x_c(t)$ is uniformly bounded in time, we obtain the desired convergence (4.17). □

**Remark 4.3.** It follows from Theorem 3.2 and Corollary 4.1 that

$$\lim_{t\to\infty}\left|x_c^j(t) - \left(\frac{1}{2}\alpha_1\cos(\omega t) + \frac{1}{2}\alpha_2\sin(\omega t)\right)\right| = 0, \quad j = 1, 2.$$

## 5. The multi-component GPL system

In this section, we study emergent dynamics to the multi-component GPL system. In the following three subsections, we will provide proofs for Theorems 3.3, 3.4 and 3.5. For this, we basically use the two-point correlation approach based on $h_{ij}$ using the explicit dynamics given in Lemma 2.2. Before we present our estimates, we introduce the following Grönwall-type lemma.

**Lemma 5.1.** *Let $y = y(t)$ be a nonnegative $\mathcal{C}^1$-function satisfying the following Riccati-type differential inequality:*

$$\dot{y} \le -py + qy^2 + r, \quad p, q, r > 0, \quad t > 0. \tag{5.1}$$

(1) *Suppose that $r = 0$. Then, $y$ satisfies the following estimate:*

$$y(t) \le \frac{1}{\left(\frac{1}{y(0)} - \frac{q}{p}\right)e^{pt} + \frac{q}{p}}, \quad t \ge 0.$$

(2) *Suppose that*

$$r > 0, \quad p^2 - 4qr > 0 \quad \text{and} \quad y(0) < y_+.$$

*Then, there exists a finite entrance time $T_*$ such that*

$$y(t) < y_-, \quad t > T_*,$$

*where $y_\pm$ are two distinct positive roots of the quadratic equation $qy^2 - py + r = 0$:*

$$y_- := \frac{p - \sqrt{p^2 - 4qr}}{2q}, \quad y_+ := \frac{p + \sqrt{p^2 - 4qr}}{2q}.$$

**Proof.** (i) We set $u = 1/y$, derive the inequality for $u$ and integrate the resulting relation to find the desired estimate.
(ii) For the proof of the second assertion, we split the proof into two cases:

$$\text{Either} \quad y(0) \le y_- \quad \text{or} \quad y_- < y(0) < y_+.$$

◇ Case A: Suppose that $y(0) \in (0, y_-]$. For the time $t = T$ such that $y(T) = y_-$, it follows from (5.1) that

$$\frac{d}{dt}y(t)\Big|_{t=T} \le 0.$$

This yields that $y(t)$ is non-increasing at time $t = T$. Hence, $y(t)$ is restricted in the interval $[0, y_-]$ for all time. Hence, one has

$$y(t) \le y_-, \quad t \ge 0.$$

⋄ Case B: Suppose that $y(0) \in (y_-, y_+)$. Since the initial datum belong to this region, we know that $y(t)$ starts to decrease strictly. Then, it follows from Proposition 3.1 in [52] that there exists a finite entrance time $T_*$ such that

$$y(t) < y_-, \quad t \ge T_*.$$

Finally, we combine Cases A and B to complete the proof. □

### 5.1. Complete synchronization

First, we recall the setting for the complete synchronization in Theorem 3.3.

$$\kappa > 0, \quad D(V) = 0, \quad \mathcal{B} = \beta J_N, \quad \lambda(\mathcal{A}) > 0, \quad \mathcal{S}(H^0) < \frac{\lambda(\mathcal{A})}{\|\mathcal{A}\|_\infty}.$$

Then, it follows from Lemma 2.2 that

$$\begin{aligned}\frac{d}{dt}(1-h_{ij}) &= -\frac{\kappa}{2}(d_i^{\mathrm{av}}(\mathcal{A}) + d_j^{\mathrm{av}}(\mathcal{A}))(1-h_{ij}) \\ &\quad + \frac{\kappa}{2N}\sum_{k=1}^N \Big( a_{ik}(1-h_{ik})(1-h_{ij}) + a_{jk}(1-h_{kj})(1-h_{ij}) \\ &\quad + (a_{ik}-a_{jk})\big((1-h_{kj}) - (1-h_{ik})\big) \Big).\end{aligned} \tag{5.2}$$

We multiply (5.2) with $1 - \bar{h}_{ij}$ and take real parts of both sides to obtain

$$\begin{aligned}\frac{1}{2}\frac{d}{dt}|1-h_{ij}|^2 &= -\frac{\kappa}{2}(d_i^{\mathrm{av}}(\mathcal{A}) + d_j^{\mathrm{av}}(\mathcal{A}))|1-h_{ij}|^2 \\ &\quad + \frac{\kappa}{2N}\sum_{k=1}^N \mathrm{Re}\Big( a_{ik}(1-h_{ik})|1-h_{ij}|^2 + a_{jk}(1-h_{kj})|1-h_{ij}|^2 \\ &\quad + (a_{ik}-a_{jk})\big((1-h_{kj}) - (1-h_{ik})\big)(1-\bar{h}_{ij}) \Big).\end{aligned}$$

For each time $t$, we choose the indices $(i_t, j_t)$ such that

$$\mathcal{S}(H(t)) := |1 - h_{i_t j_t}(t)|, \quad t \ge 0.$$

Then, $\mathcal{S}(H(t))$ satisfies the differential inequality:

$$\frac{d}{dt}\mathcal{S}(H(t)) \le -\kappa\lambda(\mathcal{A})\mathcal{S}(H(t)) + \kappa\|\mathcal{A}\|_\infty \mathcal{S}(H(t))^2, \quad t > 0.$$

Finally, we use Lemma 5.1 to derive exponential decay of $\mathcal{S}(H(t))$:

$$\mathcal{S}(H(t)) \le \frac{1}{\left(\frac{1}{\mathcal{S}(H^0)} - \frac{\lambda(\mathcal{A})}{\|\mathcal{A}_\infty\|}\right)e^{\kappa\lambda(\mathcal{A})t} + \frac{\lambda(\mathcal{A})}{\|\mathcal{A}_\infty\|}} \le \mathcal{O}(1)e^{-\kappa\lambda(\mathcal{A})t}.$$

This shows the desired exponential decay of $\mathcal{S}(H)$ and completes the proof of Theorem 3.3.

### 5.2. Practical synchronization I

Let $\psi_j = \psi_j(x,t)$ be a global smooth solution to (2.3) satisfying a priori condition,

$$\sup_{0\le t\le T}\max_j \|\psi_j(t)\|_4 \le M(T) < \infty.$$

and framework:

$$T \in (0,\infty), \quad \kappa > 0, \quad \lambda(\mathcal{A}) > 0, \quad D(V) < D(\Sigma), \quad \|\Sigma\|_\infty < \frac{\kappa\lambda(\mathcal{A})}{16\|\mathcal{A}\|_\infty(1+M(T)^2)},$$

$$\mathcal{S}(H^0) < \frac{\kappa\lambda(\mathcal{A}) + \sqrt{\big(\kappa\lambda(\mathcal{A})\big)^2 - 8\kappa\|\mathcal{A}\|_\infty\|\Sigma\|_\infty\Big(2M(T)^4+1\Big)}}{2\kappa\|\mathcal{A}\|_\infty}.$$

Under the setting above, we again use Lemma 2.2 to get

$$\begin{aligned}
&\frac{1}{2}\frac{d}{dt}|1-h_{ij}|^2 \\
&\quad = -\frac{\kappa}{2}(d_i^{\mathrm{av}}(\mathcal{A})+d_j^{\mathrm{av}}(\mathcal{A}))|1-h_{ij}|^2 + \underbrace{\mathrm{Re}\left(\mathrm{i}(1-\bar{h}_{ij})\int_{\mathbb{R}^d}(V_i-V_j)\psi_i\bar{\psi}_j dx\right)}_{=:\mathcal{I}_{51}} \\
&\qquad + \underbrace{\mathrm{Re}\left(\mathrm{i}(1-\bar{h}_{ij})\int_{\mathbb{R}^d}(\varepsilon_j|\psi_j|^2-\varepsilon_i|\psi_i|^2)\psi_i\bar{\psi}_j dx\right)}_{=:\mathcal{I}_{52}} \\
&\qquad + \frac{\kappa}{2N}\sum_{k=1}^{N}\mathrm{Re}\Big(a_{ik}(1-h_{ik})|1-h_{ij}|^2 + a_{jk}(1-h_{kj})|1-h_{ij}|^2 \\
&\qquad\qquad + (a_{ik}-a_{jk})((1-h_{kj})-(1-h_{ik}))(1-\bar{h}_{ij})\Big).
\end{aligned} \tag{5.3}$$

Note that the terms in the R.H.S. of (5.3) other than $\mathcal{I}_{51}$ and $\mathcal{I}_{52}$ are already treated in Section 5.1. Hence, we focus on the terms $\mathcal{I}_{5i},\ i=1,2$ as follows.

- (Estimate of $\mathcal{I}_{51}$): We use $\|\psi_i\|=1$ and $|1-\bar{h}_{ij}|=|1-h_{ij}|$ to see

$$|\mathcal{I}_{51}| = \left|\mathrm{Re}\left(\mathrm{i}(1-\bar{h}_{ij})\int_{\mathbb{R}^d}(V_i-V_j)\psi_i\bar{\psi}_j dx\right)\right| \le D(V)|1-h_{ij}|. \tag{5.4}$$

- (Estimate of $\mathcal{I}_{52}$): Note that

$$\begin{aligned}
\int_{\mathbb{R}^d}(\varepsilon_j|\psi_j|^2-\varepsilon_i|\psi_i|^2)\psi_i\bar{\psi}_j dx &= \varepsilon_j\int_{\mathbb{R}^d}(|\psi_j|^2-|\psi_i|^2)\psi_i\bar{\psi}_j dx + (\varepsilon_j-\varepsilon_i)\int_{\mathbb{R}^d}|\psi_i|^2\psi_i\bar{\psi}_j dx \\
&=: \mathcal{I}_{521}+\mathcal{I}_{522}.
\end{aligned}$$

◇ (Estimate of $\mathcal{I}_{521}$): Recall the simple inequality

$$\big||z_1|^2-|z_2|^2\big| \le |z_1-z_2|\big(|z_1|+|z_2|\big), \quad z_1,z_2\in\mathbb{C}. \tag{5.5}$$

Then, we use (5.5) to obtain an estimate of $\mathcal{I}_{521}$ as follows:

$$|\mathcal{I}_{521}| = \left|\varepsilon_j\int_{\mathbb{R}^d}(|\psi_j|^2-|\psi_i|^2)\psi_i\bar{\psi}_j dx\right| \le \quad \le 2\|\Sigma\|_\infty M(T)^4, \tag{5.6}$$

where we used Hölder's inequality:

$$\left|\int_{\mathbb{R}^d}|f|^2|g||h|dx\right| \le \left(\int_{\mathbb{R}^d}|f|^4dx\right)^{\frac{1}{2}}\left(\int_{\mathbb{R}^d}|g|^4dx\right)^{\frac{1}{4}}\left(\int_{\mathbb{R}^d}|h|^4dx\right)^{\frac{1}{4}} = \|f\|_4^2\|g\|_4\|h\|_4. \tag{5.7}$$

◇ (Estimate of $\mathcal{I}_{522}$): We use (5.7) to find an estimate of $\mathcal{I}_{522}$:

$$|\mathcal{I}_{522}| \le D(\Sigma)M(T)^4. \tag{5.8}$$

Finally, we combine (5.6) and (5.8) to estimate the term $\mathcal{I}_{52}$:

$$\begin{aligned}
|\mathcal{I}_{52}| &= \left|\mathrm{Re}\left(\mathrm{i}(1-\bar{h}_{ij})\int_{\mathbb{R}^d}(\varepsilon|\psi_j|^2-\varepsilon|\psi_i|^2)\psi_i\bar{\psi}_j dx\right)\right| \le |1-h_{ij}|(|\mathcal{I}_{521}|+|\mathcal{I}_{522}|) \\
&\le 2M(T)^4\|\Sigma\|_\infty|1-h_{ij}| + D(\Sigma)M(T)^4|1-h_{ij}|.
\end{aligned} \tag{5.9}$$

In (5.3), we combine (5.4) and (5.9) to derive a differential inequality of $\mathcal{S}(H)$:

$$\begin{aligned}
\frac{d}{dt}\mathcal{S}(H) &\le -\kappa\lambda(\mathcal{A})\mathcal{S}(H(t)) + \kappa\|\mathcal{A}\|_\infty\mathcal{S}(H(t))^2 \\
&\qquad + 2M(T)^4\|\Sigma\|_\infty + D(\Sigma)M(T)^4 + D(V), \quad t\in(0,T].
\end{aligned} \tag{5.10}$$

On the other hand, we note that

$$D(V) < D(\Sigma) < 2\|\Sigma\|_\infty. \tag{5.11}$$

Finally, we combine (5.10) and (5.11) to obtain that for $t\in(0,T]$,

$$\frac{d}{dt}\mathcal{S}(H) \le -\kappa\lambda(\mathcal{A})\mathcal{S}(H(t)) + \kappa\|\mathcal{A}\|_\infty\mathcal{S}(H(t))^2 + 2\|\Sigma\|_\infty\Big(2M(T)^4+1\Big). \tag{5.12}$$

We now apply Lemma 5.1 for (5.12) with

$$p := \kappa\lambda(\mathcal{A}), \quad q := \kappa\|\mathcal{A}\|_\infty, \quad r := 2\|\Sigma\|_\infty\Big(2M(T)^4+1\Big)$$

to get that there exists a finite time $T_1 > 0$ such that for $t > T_1$,

$$\begin{aligned}\mathcal{S}(H(t)) &< \frac{\kappa\lambda(\mathcal{A}) - \sqrt{\left(\kappa\lambda(\mathcal{A})\right)^2 - 8\kappa\|\mathcal{A}\|_\infty\|\Sigma\|_\infty\left(2M(T)^4+1\right)}}{2\kappa\|\mathcal{A}\|_\infty} \\ &= \frac{4\|\Sigma\|_\infty\left(2M(T)^4+1\right)}{\kappa\lambda(\mathcal{A}) + \sqrt{\left(\kappa\lambda(\mathcal{A})\right)^2 - 8\kappa\|\mathcal{A}\|_\infty\|\Sigma\|_\infty\left(2M(T)^4+1\right)}} \\ &= \mathcal{O}(1)\left(\frac{\|\Sigma\|_\infty\left(2M(T)^4+1\right)}{\kappa\lambda(\mathcal{A})}\right).\end{aligned}$$

This completes the proof of Theorem 3.4.

### 5.3. Practical synchronization II

Let $\psi_j$ be a global smooth solution to (2.3) satisfying a priori condition:

$$\sup_{0\le t\le T}\max_j \|\psi_j(t)\|_4 \le M(T) < \infty,$$

and recall the framework:

$$\lambda(\mathcal{A}) > 0, \quad \kappa > \frac{4G\|\Sigma\|_\infty}{(\lambda(\mathcal{A}))^2}, \quad \mathcal{S}(H^0) < \frac{\kappa\lambda(\mathcal{A}) + \sqrt{\left(\kappa\lambda(\mathcal{A})\right)^2 - 4\kappa G\|\Sigma\|_\infty}}{2\kappa\|\Sigma\|_\infty}.$$

By the same calculation as in (5.3), we have

$$\begin{aligned}&\frac{1}{2}\frac{d}{dt}|1-h_{ij}|^2 \\ &= -\frac{\kappa}{2}(d_i^{\mathrm{av}}(\mathcal{A}) + d_j^{\mathrm{av}}(\mathcal{A}))|1-h_{ij}|^2 + \mathrm{Re}\left(\mathrm{i}(1-\bar{h}_{ij})\int_{\mathbb{R}^d}(V_i - V_j)\psi_i\bar{\psi}_j dx\right) \\ &\quad + \mathrm{Re}\left[\,\mathrm{i}(1-\bar{h}_{ij})\underbrace{\int_{\mathbb{R}^d}\left((\beta_{ji}-\beta_{ii})|\psi_i|^2 + (\beta_{jj}-\beta_{ij})|\psi_j|^2 + \sum_{k\ne i,j}(\beta_{ik}-\beta_{jk})|\psi_k|^2\right)\psi_i\bar{\psi}_j dx}_{=:\mathcal{I}_6}\,\right] \\ &\quad + \frac{\kappa}{2N}\sum_{k=1}^N \mathrm{Re}\Big(a_{ik}(1-h_{ik})|1-h_{ij}|^2 + a_{jk}(1-h_{kj})|1-h_{ij}|^2 \\ &\qquad + (a_{ik}-a_{jk})((1-h_{kj}) - (1-h_{ik}))(1-\bar{h}_{ij})\Big).\end{aligned} \tag{5.13}$$

Note that the only difference between (5.3) and (5.13) is the term $\mathcal{I}_6$ which can be estimated as follows:

$$\begin{aligned}\mathcal{I}_6 &= \int_{\mathbb{R}^d}\left((\beta_{ji}-\beta_{ii})|\psi_i|^2 + (\beta_{jj}-\beta_{ij})|\psi_j|^2 + \sum_{k\ne i,j}(\beta_{ik}-\beta_{jk})|\psi_k|^2\right)\psi_i\bar{\psi}_j dx \\ &= \mathrm{i}(\beta_{ij}-\beta)\int_{\mathbb{R}^d}(|\psi_i|^2 - |\psi_j|^2)\psi_i\bar{\psi}_j dx - \varepsilon_i\int_{\mathbb{R}^d}|\psi_i|^2\psi_i\bar{\psi}_j dx + \varepsilon_j\int_{\mathbb{R}^d}|\psi_j|^2\psi_i\bar{\psi}_j dx \\ &\quad + \mathrm{i}\sum_{k\ne i,j}\int_{\mathbb{R}^d}(\beta_{ik}-\beta_{jk})|\psi_k|^2\psi_i\bar{\psi}_j dx \\ &=: \mathcal{I}_{61} + \mathcal{I}_{62} + \mathcal{I}_{63} + \mathcal{I}_{64}.\end{aligned}$$

Below, we present the estimates of $\mathcal{I}_{6k}$, $k = 1, 2, 3, 4$, respectively.

◇ (Estimate of $\mathcal{I}_{61}$): We use the inequality (5.5) and follow the same argument in (5.6) to find

$$\begin{aligned}|\mathcal{I}_{61}| &= \left|\mathrm{i}(\beta_{ij}-\beta)\int_{\mathbb{R}^d}(|\psi_i|^2 - |\psi_j|^2)\psi_i\bar{\psi}_j dx\right| \le R(\mathcal{B})\int_{\mathbb{R}^d}\left||\psi_i|^2 - |\psi_j|^2\right||\psi_i||\psi_j| dx \\ &\le 2M(T)^4 R(\mathcal{B}).\end{aligned} \tag{5.14}$$

◇ (Estimate of $\mathcal{I}_{62} + \mathcal{I}_{63}$): We use a priori estimate (5.12) to get

$$|\mathcal{I}_{62} + \mathcal{I}_{63}| = \left|-\varepsilon_i\int_{\mathbb{R}^d}|\psi_i|^2\psi_i\bar{\psi}_j dx + \varepsilon_j\int_{\mathbb{R}^d}|\psi_j|^2\psi_i\bar{\psi}_j dx\right| \le 2M(T)^4\|\Sigma\|_\infty.$$

◇ (Estimate of $\mathcal{I}_{64}$): Similar to the estimate of $\mathcal{I}_{62} + \mathcal{I}_{63}$, we have

$$|\mathcal{I}_{64}| = \left|\mathrm{i}\sum_{k\ne i,j}\int_{\mathbb{R}^d}(\beta_{ik}-\beta_{jk})|\psi_k|^2\psi_i\bar{\psi}_j dx\right| \le 2\delta(\mathcal{B})M(T)^4. \tag{5.15}$$

In (5.13), we combine (5.14)–(5.15) to obtain

$$\frac{d}{dt}\mathcal{S}(H) \le -\kappa\lambda(\mathcal{A})\mathcal{S}(H(t)) + \kappa\|\mathcal{A}\|_\infty \mathcal{S}(H(t))^2 + \underbrace{2M(T)^4(R(\mathcal{B}) + \|\Sigma\|_\infty + \delta(\mathcal{B})) + D(V)}_{=:G}, \quad t \in (0, T],$$

where we used definition of $G$ in (3.9).

Now we apply Lemma 2.2 with

$$p := \kappa\lambda(\mathcal{A}), \quad q := \kappa\|\mathcal{A}\|_\infty, \quad r := G,$$

to derive that there exists a finite entrance time $T_2$ such that for $t > T_2$,

$$\mathcal{S}(H(t)) \le \frac{\kappa\lambda(\mathcal{A}) - \sqrt{\left(\kappa\lambda(\mathcal{A})\right)^2 - 4\kappa G\|\Sigma\|_\infty}}{2\kappa\|\Sigma\|_\infty} = \frac{2G}{\kappa\lambda(\mathcal{A}) + \sqrt{\left(\kappa\lambda(\mathcal{A})\right)^2 - 4\kappa G\|\Sigma\|_\infty}} \le \frac{2G}{\kappa\lambda(\mathcal{A})}.$$

Therefore, we can obtain the desired estimate and this completes the proof.

## 6. Numerical simulations

In this section, we propose an efficient and accurate numerical method for discretizing the GPL system (1.2). Several numerical examples will be carried out and compared with those analytical results shown in previous sections. Due to the external trapping potential $V_j(x)$ $(j = 1, \dots, N)$, the wave functions $\psi_j$ $(j = 1, \dots, N)$ decay exponentially as $|x| \to \infty$. Therefore, it suffices to truncate the problem (1.2) into a sufficiently large bounded domain $\mathcal{D} \subset \mathbb{R}^d$ with periodic boundary condition (BC). The bounded domain $\mathcal{D}$ is chosen as a box $[a, b] \times [c, d] \times [e, f]$ in 3D, a rectangle $[a, b] \times [c, d]$ in 2D, and an interval $[a, b]$ in 1D.

### *6.1. A time splitting Crank–Nicolson spectral method*

Choose $\Delta t > 0$ as the time step size and denote time steps $t_n := n\Delta t$ for $n \ge 0$. From time $t = t_n$ to $t = t_{n+1}$, the GPL will be solved in three splitting steps. One solves first

$$\mathrm{i}\partial_t \psi_j = -\frac{1}{2}\Delta\psi_j, \quad x \in \mathcal{D}, \quad j = 1, \dots, N, \tag{6.1}$$

with periodic BC on the boundary $\partial\mathcal{D}$ for the time step of length $\Delta t$, then solves

$$\mathrm{i}\partial_t \psi_j = V_j\psi_j + \sum_{k=1}^N \beta_{jk}|\psi_k|^2\psi_j, \quad j = 1, \dots, N, \tag{6.2}$$

for the same time step, and then solves

$$\mathrm{i}\partial_t \psi_j = \frac{\mathrm{i}\kappa}{2N}\sum_{k=1}^N a_{jk}\left(\psi_k - \frac{\langle\psi_j, \psi_k\rangle}{\langle\psi_j, \psi_j\rangle}\psi_j\right), \quad j = 1, \dots, N, \tag{6.3}$$

for the same time step. The linear subproblem (6.1) will be discretized in space by the Fourier pseudospectral method and integrated in time analytically in the phase space [6,10,11,44]. For the nonlinear subproblem (6.2), it conserves $|\psi_k|^2$ point-wisely in time, i.e. $|\psi_k(x, t)|^2 \equiv |\psi_k(x, t_n)|^2$ for $t_n \le t \le t_{n+1}$ and $k = 1, \dots, N$ [6,10,11,44]. Thus it collapses to a linear subproblem and can be integrated in time analytically [6,10,11,44]. For the nonlinear subproblem (6.3), due to the presence of the Lohe term, it cannot be integrated analytically (or explicitly) in the way for the standard GPE [6,44]. Therefore, we will apply a Crank–Nicolson scheme to further discretize the temporal derivate of (6.3) [8].

To simplify the presentation, we will only present the scheme for 1D. Generation to $d > 1$ is straightforward for tensor grids. To this end, we choose the spatial mesh size as $\Delta x = \frac{b-a}{M}$ with $M$ a even positive integer, and let the grid points be

$$x_\ell = a + \ell\Delta x, \qquad \ell = 0, \dots, M.$$

For $1 \le j \le N$ denote $\psi_{j,\ell}^n$ as the approximation of $\psi_j(x_\ell, t_n)$ $(0 \le \ell \le M)$ and $\boldsymbol{\psi}_j^n$ as the solution vector with component $\psi_{j,\ell}^n$. Combining the time splitting (6.1)–(6.3) via the Strang splitting and the Crank–Nicolson scheme for (6.3), a second order *Time Splitting Crank–Nicolson Fourier Pseudospectral* (TSCN–FP) method to solve GPL on $\mathcal{D}$ reads as:

$$\psi_{j,\ell}^{(1)} = \sum_{p=-M/2}^{M/2-1} e^{-i\Delta t\,\mu_p^2/4}\,\widehat{(\boldsymbol{\psi}_j^n)}_p\, e^{i\mu_p(x_\ell - a)},$$

$$\psi_{j,\ell}^{(2)} = e^{-i\Delta t\left(V_j(x_\ell) + \sum_{k=1}^N \beta_{jk}|\psi_{k,\ell}^{(1)}|^2\right)/2}\,\psi_{j,\ell}^{(1)},$$

$$
\begin{aligned}
i\frac{\psi_{j,\ell}^{(3)}-\psi_{j,\ell}^{(2)}}{\Delta t} &= \frac{i\kappa}{2N}\sum_{k=1}^{N} a_{jk}\left[\psi_{k,\ell}^{(\frac{5}{2})}-\frac{\langle \boldsymbol{\psi}_j^{(\frac{5}{2})},\boldsymbol{\psi}_k^{(\frac{5}{2})}\rangle_{\Delta x}}{\langle \boldsymbol{\psi}_j^{(\frac{5}{2})},\boldsymbol{\psi}_j^{(\frac{5}{2})}\rangle_{\Delta x}}\,\psi_{j,\ell}^{(\frac{5}{2})}\right], \\
\psi_{j,\ell}^{(4)} &= e^{-i\Delta t\left(V_j(x_\ell)+\sum_{k=1}^{N}\beta_{jk}|\psi_{k,\ell}^{(3)}|^2\right)/2}\,\psi_{j,\ell}^{(3)}, \quad 0\le \ell\le M, \quad 1\le j\le N, \\
\psi_{j,\ell}^{n+1} &= \sum_{p=-M/2}^{M/2-1} e^{-i\Delta t\,\mu_p^2/4}\,\widehat{(\boldsymbol{\psi}_j^{(4)})}_p\, e^{i\mu_p(x_\ell-a)}.
\end{aligned}
\tag{6.4}
$$

Here, $\mu_p = \frac{p\pi}{b-a}$, $\widehat{(\boldsymbol{\psi}_j^{n})}_p$ and $\widehat{(\boldsymbol{\psi}_j^{(4)})}_p$ ($p = -\frac{M}{2},\dots,\frac{M}{2}$) are the discrete Fourier transform coefficients of the vectors $\boldsymbol{\psi}_j^n$ and $\boldsymbol{\psi}_j^{(4)}$ ($j = 1,\dots,N$), respectively. Moreover,

$$
\psi_{j,\ell}^{(\frac{5}{2})} =: \frac{1}{2}\left(\psi_{j,\ell}^{(3)}+\psi_{j,\ell}^{(2)}\right), \qquad \langle \boldsymbol{\psi}_j^{(\frac{5}{2})},\boldsymbol{\psi}_k^{(\frac{5}{2})}\rangle_{\Delta x} =: \Delta x\sum_{\ell=0}^{M-1}\psi_{j,\ell}^{(\frac{5}{2})}\,\bar{\psi}_{k,\ell}^{(\frac{5}{2})}.
$$

Although the Crank–Nicolson step (6.4) is fully implicit, it can be either solved efficiently by Krylov subspace iteration method with proper preconditioner [53] or the fixed-point iteration method with a stabilization parameter [54]. In addition, TSCN–FP is of spectral accuracy in space and second-order accuracy in time. By following the standard procedure, it is straightforward to show that the TSCN–FP conserve mass of each component in discrete level, i.e., $\|\boldsymbol{\psi}_j^n\|_{l^2}^2 := \langle \boldsymbol{\psi}_j^n,\boldsymbol{\psi}_j^n\rangle_{\Delta x} \equiv \|\boldsymbol{\psi}_j^0\|_{l^2}^2$ for $n\ge 0$ and $j = 1, 2,\dots,N$. We omit the details here for brevity.

## 6.2. Numerical results

In this section, we apply the TSCN–FP schemes proposed in the previous section to simulate some interesting dynamics. For our simulation, we choose

$$
\beta = 1, \quad \Delta t = 2\times 10^{-4}, \quad \mathcal{D} = [-12, 12]^d, \quad d = 1, 2.
$$

The potentials and initial data are chosen respectively as follows:

$$
V_j(x) = \pi^2\alpha_j^2\,|x|^2, \quad \psi_j^0 = \sqrt{a_j/\pi}\; e^{-a_j|x-x_0^j|^2}.
$$

Here, $\alpha_j$ and $x_0^j$ are real constants that will be given later. In fact, complete and practical synchronization estimates do not depend on the form of the initial data and the relative $L^2$-distances of the initial data play a crucial role. However, when we deal with the center-of-mass $x_c$, we used the Gaussian initial data so that they have the symmetric form (see Remark 4.2).

**Example 6.1.** Here, we consider the two-component system in 1-d, i.e., we take $N = 2$ and $d = 1$ in (1.2). To this end, we take $(x_1^0, x_2^0) = (2.5, -5)$ and consider the following two cases: for $j = 1, 2$

**Case 1.** fix $\alpha_j = \beta_{j\ell} = 1$ ($\ell = 1, 2$) and vary $\kappa = 0, 2, 20$.
**Case 2.** fix $\alpha_j = j$, $\beta_{12} = \beta_{21} = 1$, $\beta_{11} = 4\beta_{22} = 2$ and vary $\kappa = 0, 2, 10, 20$.

Figs. 6.1 and 6.2 depict the time evolution of the quantity $1 - R(t)$ (where $R(t)$ is the real part of the correlation function $h_{12}(t)$), the center of mass $x_c^j(t)$, the component mass $\|\psi_j\|^2$ and the total energy $\mathcal{E}(t)$ for **Case 1** and **Case 2**, respectively. From these figures and other numerical experiments not shown here for brevity, we can see the following observations.
(i) For all cases, we observe that the mass is conserved along time.
(ii) If the Lohe coupling is off, i.e., $\kappa = 0$, both the mass and energy are conserved well, and the center of mass $(x_c^1(t), x_c^2(t))$ is periodic in time with the same period. In addition, for the identical case, i.e., $\mathcal{B} = J_2$ and $V_1(x) = V_2(x)$, $R(t)$ is conserved for identical case.
(iii) If the Lohe coupling is on, i.e., $\kappa > 0$, the phenomena become complicated. The energy is no longer conserved, indeed it decays to some value for large $\kappa$ while oscillates for small $\kappa$.
(iv) Moreover, for the identical case, $R(t)$ converges exponentially to 1, which coincides with the theoretical results. Thus, the complete synchronization occurs in this case. After the complete synchronization, $\|\psi_1(x,t) - \psi_2(x,t)\|_\infty$ will converge to zero and the center of mass $x_c^1(t)$ and $x_c^2(t)$ will become the same and swing periodically along the line connecting $-\bar{x}_c^0$ and $\bar{x}_c^0$ (here, $\bar{x}_c^0 := (x_c^1(0) + x_c^2(0))/2$).
(v) Furthermore, for the non-identical case, i.e., $\mathcal{B} \ne J_2$ and $V_1(x) \ne V_2(x)$, $R(t)$ does not converge to 1, i.e., the complete synchronization cannot occur. However, for large $\kappa$, $R(t)$ indeed converges to some definite constant $R_\infty < 1$. The larger $\kappa$, the smaller value $1 - R_\infty$. Meanwhile, $|x_c^1(t) - x_c^2(t)|$ also converges to zero, which could be also justified in a similar process as shown in Corollary 4.1.

**Example 6.2.** Here, we consider the six-component system in 2-d, i.e., we take $N = 6$ and $d = 2$ in (1.2). To this end, we here only consider the identical case, i.e., we choose $\alpha_j = 1 = \beta_{j\ell} = 1$ ($j, \ell = 1,\dots,6$ ). Let $\kappa = 20$, we consider four cases of initial setups:

**Case 3.** $x_0^j = \big(6\cos((j-1)\pi/3), 6\sin((j-1)\pi/3)\big), \quad j = 1,\dots,6.$
**Case 4.** $x_0^j = \big(2 + 4\cos(j\pi/3 - \pi/12), 2 + 4\sin(j\pi/3 - \pi/12)\big), \quad j = 1,\dots,6.$
**Case 5.** $x_0^j = \big(6\cos((j-1)\pi/5), 6\sin((j-1)\pi/5)\big), \quad j = 1,\dots,6.$
**Case 6.** Random location:

$$
\begin{aligned}
&x_0^1 = (3.4707, 2.7526), \quad x_0^2 = (-0.8931, 1.9951), \quad x_0^3 = (0.1809, -1.1538),\\
&x_0^4 = (0.0937, -5.8995), \quad x_0^5 = (-2.9235, -2.4171), \quad x_0^6 = (-3.6423, 4.3714).
\end{aligned}
$$

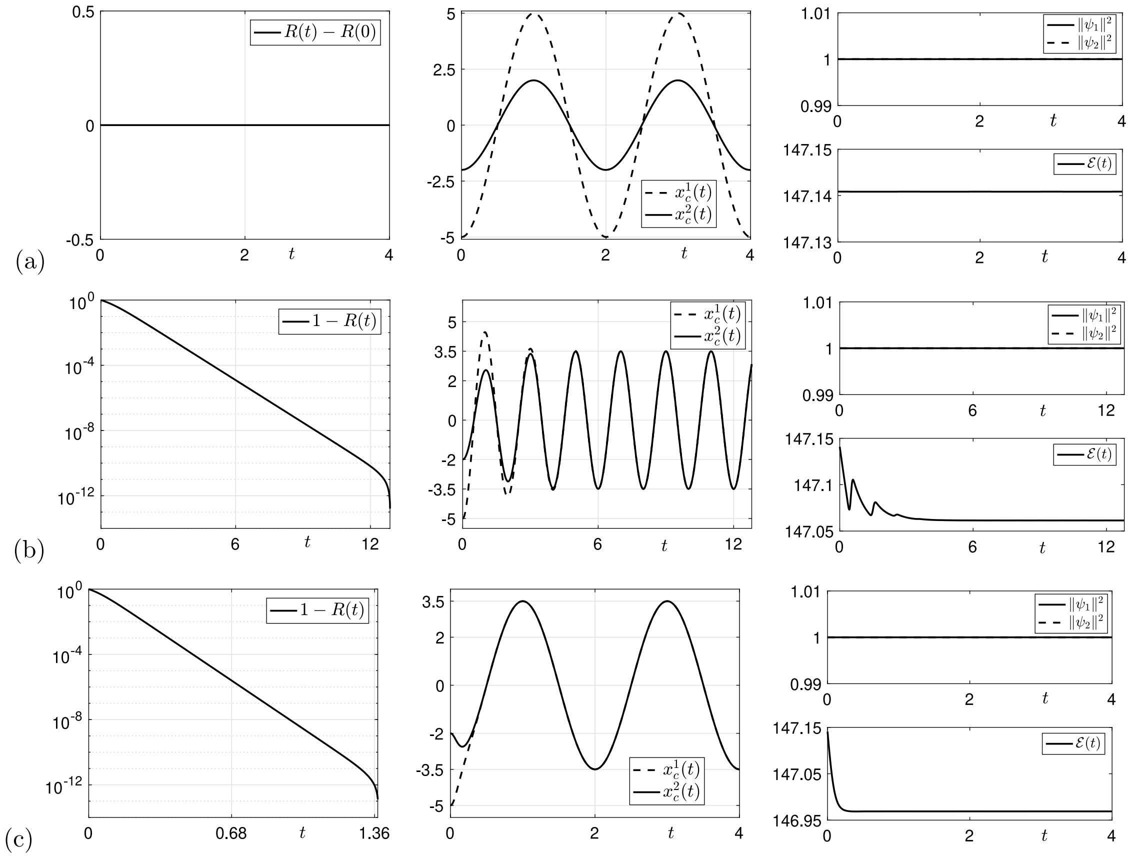


**Fig. 6.1.** Time evolution of the quantity $1 - R(t)$ (left), the center of mass $x_c^j(t)$ (middle), and the component mass $\|\psi_j\|^2$ and the total energy $\mathcal{E}(t)$ (right) for **Case 1** in Example 6.1 for $\kappa = 0, 2, 20$ (top to bottom).

For **Cases 3–6**, Fig. 6.3 illustrates the trajectory and time evolution of the center of mass $x_c^j(t) =: (x_{c1}^j(t), x_{c2}^j(t))$, Fig. 6.4 depicts the time evolution of $|\mathcal{R}_{1256}(t) - \mathcal{R}_{1256}(0)|$, $|\mathcal{R}_{2456}(t) - \mathcal{R}_{2456}(0)|$ & $|\mathcal{R}_{3456}(t) - \mathcal{R}_{3456}(0)|$, and Fig. 6.5 shows the contour plots of $|\psi_1(x, t)|^2$ at different times for. From these figures and other numerical experiments not shown here for brevity, we can see the following observations.

(i) The complete synchronization occurs for all cases.

(ii) All the center of mass $x_c^j(t)$ $(j = 1, \dots, 6)$ will converge to the same periodic function $\bar{x}_c(t)$, which swings exactly along the line connecting the points $(-\bar{x}_{c1}^0, -\bar{x}_{c2}^0)$ and $(\bar{x}_{c1}^0, \bar{x}_{c2}^0)$ which are defined as the average of the initial center of mass of the six oscillators:

$$\left(\bar{x}_{c1}^0, \bar{x}_{c2}^0\right) := \left(\frac{1}{6}\sum_{j=1}^{6} x_{c1}^j(0), \ \frac{1}{6}\sum_{j=1}^{6} x_{c2}^j(0)\right).$$

Thus, when $\bar{x}_{c1}^0 = \bar{x}_{c2}^0 = 0$, the center of mass will stay steady at the origin (cf. Fig. 6.3(a)), which also agrees with the conclusion in Remark 4.2.

(iii) Before synchronization, all density profiles $|\psi_j(x, t)|^2$ $(j = 1, \dots, 6)$ will evolve similarly, i.e., the same dynamical pattern as those shown in Fig. 6.5 for $|\psi_1|^2$ (only differ from the 'color', i.e., the more blurred humps imply the centers of the other five components, while the lighter one shows the one of the current component). While after synchronization (around $t = 0.4$, which corresponds to the moment the center of mass $x_c^j$ $(j = 1, \dots, 6)$ meet together in Fig. 6.3), all $\psi_j(x, t)$ (hence also for all density profiles) will converge to the same function, whose density changes periodically in time (as shown in columns 4–6 in Fig. 6.5, which also indicate the periodic dynamics for the center of mass that illustrated in Fig. 6.3). In addition, before synchronization, although the numerical schemes cannot conserve the cross-ratio like quantities $\mathcal{R}_{ijkl}(t)(1 \le i, j, k, l \le 6)$ in discretized level, the difference of those quantities from their initial ones is still small (cf. Fig. 6.4). It would be interesting problem to derive numerical schemes which preserve those quantities exactly in discretized level, and we leave it here as a future work in [55].

## 7. Conclusion

In this paper, we have proposed coupled nonlinear Schrödinger equations, namely the Gross–Pitaevskii–Lohe (GPL) system. This model incorporates the nonlinear cubic interactions between quantum particles for BEC and nonlinear Lohe interactions for quantum synchronization. We provided several sufficient frameworks for complete and practical synchronizations of the GPL system. For the analytical treatment, we considered three types of interaction matrices for cubic interactions: fully identical, weakly identical and

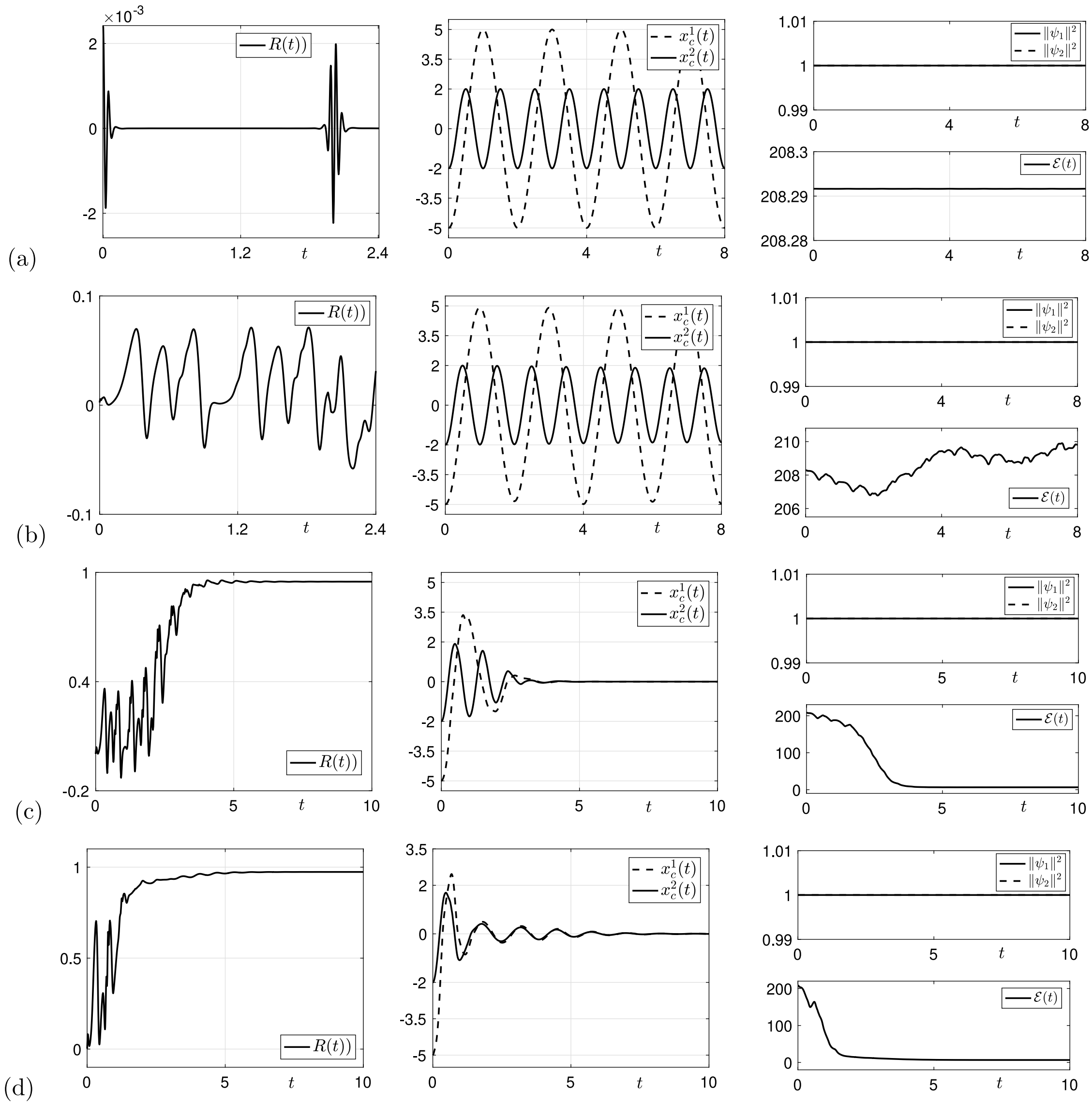

**Fig. 6.2.** Time evolution of the quantity $1 - R(t)$ (left), the center of mass $x_c^j(t)$ (middle), and the component mass $\|\psi_j\|^2$ and the total energy $\mathcal{E}(t)$ (right) for **Case 2** in Example 6.1 for $\kappa = 0, 2, 10, 20$ (top to bottom).

heterogeneous cases. For the fully identical case where interaction rates are the same constant, we presented a sufficient framework leading to the complete synchronization in terms of the system parameters and initial data. We here assumed that the network matrix is close to the identity matrix in $L^\infty$-topology. For the weakly and fully nonidentical cases, we have shown that practical synchronization can emerge in any finite time interval when the perturbation of the interaction matrix around the common positive constant is sufficiently small or the coupling strength between oscillators is sufficiently large. Since we do not know whether $L^4$-norm of a wavefunction is uniformly-in-time bounded or not, we provide the estimate which is valid on any finite time interval. On the other hand, for the two-oscillator system, we provided explicit dynamic laws for the governing law of the motion of the center-of-mass. In this case, we have observed that both periodic behavior and synchronous behavior can emerge under some well-prepared initial data. On the numerical front, we fully discretize the GPL system by utilizing Fourier pseudo-spectral in space and time-splitting scheme coupled with Crank–Nicolson scheme in time. Applying these methods, we presented several numerical examples supporting our analytic results. There are many interesting issues which are not addressed in this paper, e.g., existence of stationary states and their stability. We leave these issues as future works.

## Appendix A. Proof of Theorem 3.1

In this appendix, we present global well-posedness of system (1.2):

$$\begin{cases} \mathrm{i}\partial_t \psi_j = -\frac{1}{2}\Delta\psi_j + V_j\psi_j + \sum_{k=1}^{N} \beta_{jk}|\psi_k|^2\psi_j + \frac{\mathrm{i}\kappa}{2N}\sum_{k=1}^{N} a_{jk}\left(\psi_k - \frac{\langle\psi_j, \psi_k\rangle}{\langle\psi_j, \psi_j\rangle}\psi_j\right), \\ \psi_j(x, 0) = \psi_j^0(x), \quad (x, t) \in \mathbb{R}^d \times \mathbb{R}_+, \quad j = 1, \ldots, N. \end{cases} \tag{A.1}$$

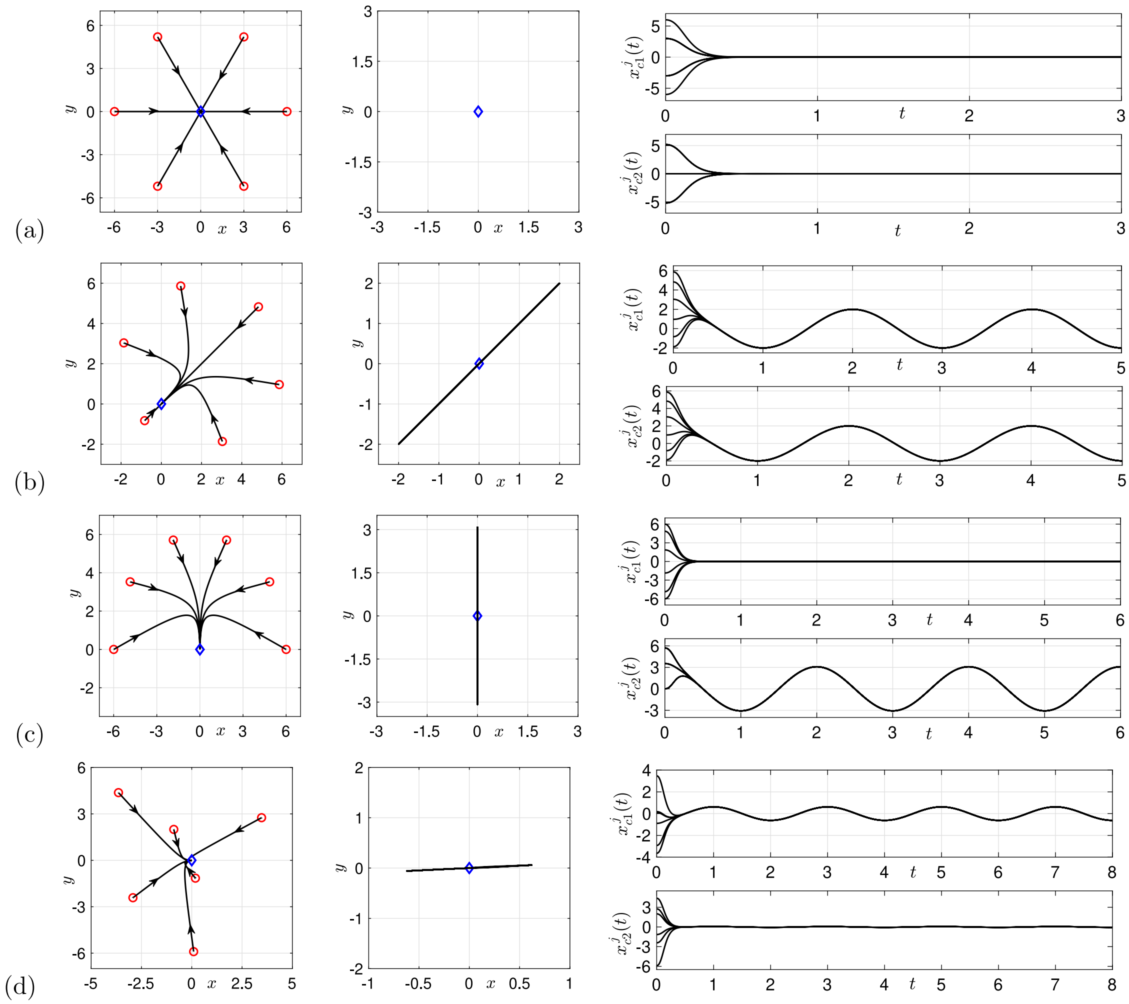


**Fig. 6.3.** First two columns: trajectory of center of mass $x_c^j(t)$ in $t \in [0, t_c]$ and $t \in [t_c, 10]$ ($t_c = 1.5$ for first row while 0.5 for the others). The third column: time evolution of $x_{c1}^j(t)$ and $x_{c2}^j(t)$ (right). $\circ$ denotes location of $x_c^j(0)$, while $\diamond$ denotes the one of $x_c^j(t_c)$.

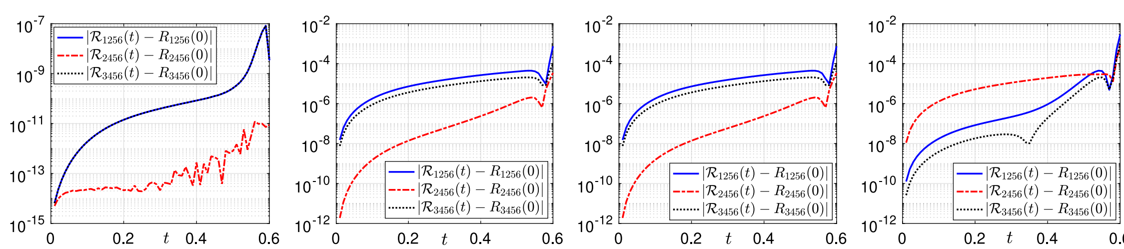


**Fig. 6.4.** Time evolution of $|\mathcal{R}_{1256}(t) - \mathcal{R}_{1256}(0)|$, $|\mathcal{R}_{2456}(t) - \mathcal{R}_{2456}(0)|$ and $|\mathcal{R}_{3456}(t) - \mathcal{R}_{3456}(0)|$ for **Case** 3–6 (Left to right).

### *A.1. Strichartz estimates*

We first recall the classical Strichartz estimates (see for instance Theorem 2.3.3 in [56]). Let $\mathcal{U}(t) = e^{\frac{i}{2}t\Delta}$ be a Schrödinger group generated by the Laplacian, and we say that a pair $(q, r)$ is *admissible* if

$$\begin{cases} 2 \le r \le \infty, & d = 1, \\ 2 \le r < \infty, & d = 2, \\ 2 \le r \le \dfrac{2d}{d-2}, & d \ge 3, \end{cases} \qquad \text{and} \quad \frac{2}{q} = d\left(\frac{1}{2} - \frac{1}{r}\right).$$

**Proposition A.1** (*Strichartz Estimates*). *The following assertions hold:*
*(i) For every $\varphi \in L^2(\mathbb{R}^d)$, the function $t \mapsto U(t)\varphi$ belongs to*

$$L^q(\mathbb{R}, L^r(\mathbb{R}^d)) \cap C(\mathbb{R}, L^2(\mathbb{R}^d))$$

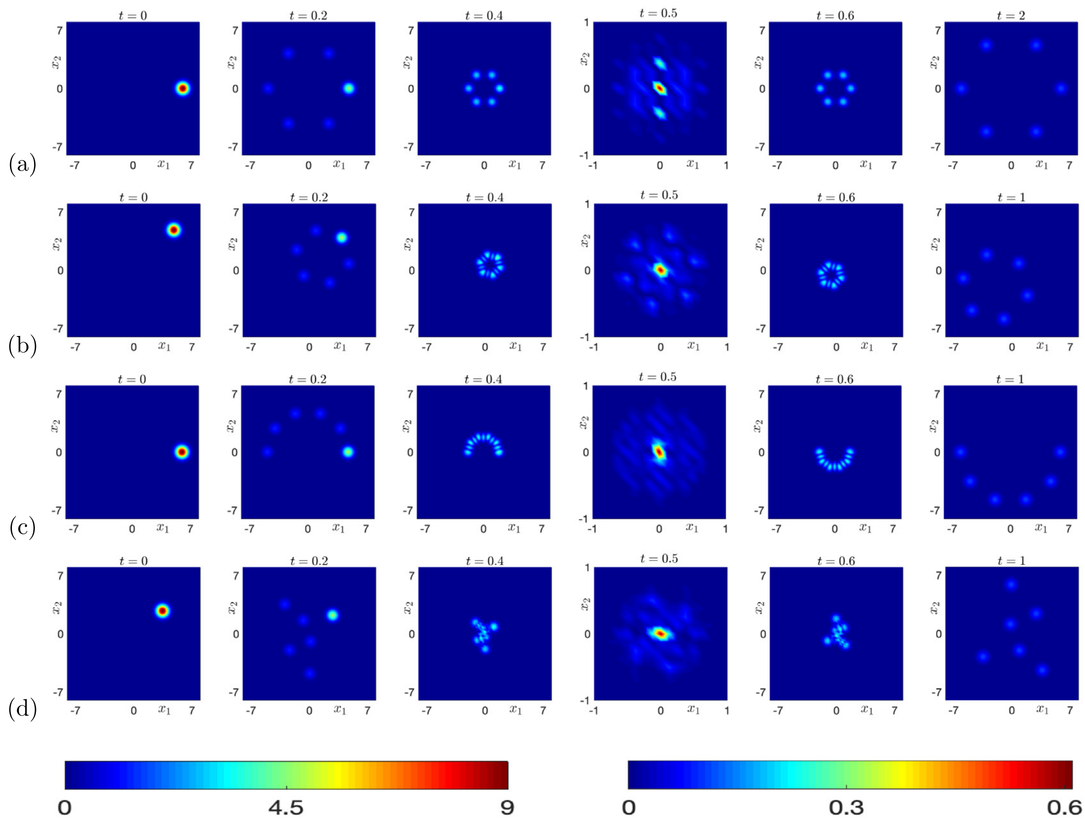

**Fig. 6.5.** Contour plots of $|\psi_1(x,t)|^2$ at different time $t$ for **Cases 3–5** in Example 6.2 (the top 4 rows) and color bars of the contour plots at $t = 0.5$ (bottom left) and other time $t$ (bottom right).

*for every admissible pair* $(q, r)$*. Furthermore, there exists a constant* $C$ *such that*

$$\|\mathcal{U}(\cdot)\varphi\|_{L^q(\mathbb{R},L^r)} \le C\|\varphi\|_{L^2(\mathbb{R}^d)} \quad \text{for every } \varphi \in L^2(\mathbb{R}^d).$$

*(ii) Let* $I$ *be an interval of* $\mathbb{R}$ *and* $t_0 \in \bar{I}$*. If* $(\gamma, \rho)$ *is an admissible pair and* $f \in L^{\gamma'}(I, L^{\rho'}(\mathbb{R}^d))$*, then for every admissible pair* $(q, r)$*, the function*

$$t \mapsto \Phi_f(t) = \int_{t_0}^{t} \mathcal{U}(t-s)f(s)ds, \quad t \in I$$

*belongs to* $L^q(I, L^r(\mathbb{R}^d)) \cap C(\bar{I}, L^2(\mathbb{R}^d))$*. Furthermore, there exists a constant* $C$ *independent of* $I$ *such that*

$$\|\Phi_f\|_{L^q(I,L^r)} \le C\|f\|_{L^{\gamma'}(I,L^{\rho'})} \quad \text{for every } f \in L^{\gamma'}(I, L^{\rho'}(\mathbb{R}^d)).$$

Below, we introduce the energy space for an external harmonic potential:

$$X_H := \left\{u \in H^1(\mathbb{R}^d) \ : \ x \mapsto |x|u(x) \in L^2(\mathbb{R}^d)\right\},$$

where the norm $\|\cdot\|_{X_H}$ associated to $X_H$ is defined as follows:

$$\|u\|_{X_H} := \|u\|_{L^2(\mathbb{R}^d)} + \|\nabla u\|_{L^2(\mathbb{R}^d)} + \|xu\|_{L^2(\mathbb{R}^d)}.$$

We first show the local existence for (A.1).

**Lemma A.1** (*Local Existence*)**.** *Suppose that the initial data belongs to* $X_H$*:*

$$\psi_j^0 \in X_H \quad \text{for all } j = 1, \dots, N.$$

*Then, there exist* $T_*$ *and a unique solution to* (A.1) *such that*

$$\psi_j, \nabla\psi_j, x\psi_j \in C([0,T]; L^2(\mathbb{R}^d)) \cap L^{\frac{8}{d}}([0,T]; L^4(\mathbb{R}^d)).$$

**Proof.** We use Duhamel's formula for (A.1) to find

$$\begin{aligned}\psi_j(t) &= \mathcal{U}(t)\psi_j^0 + \int_0^t \mathcal{U}(t-s)(V_j\psi_j(s))\,ds + \int_0^t \mathcal{U}(t-s)\left(\sum_{k=1}^N \beta_{jk}|\psi_k|^2\psi_j\right)ds \\ &\quad + \frac{\mathrm{i}\kappa}{2N}\sum_{k=1}^N a_{jk}\underbrace{\int_0^t \mathcal{U}(t-s)\left(\psi_k - \frac{\langle\psi_j,\psi_k\rangle}{\langle\psi_j,\psi_j\rangle}\psi_j\right)ds}_{=:\,\mathcal{I}_7}, \quad t\in[0,T].\end{aligned} \tag{A.2}$$

The first three terms in the right-hand side of (A.2) can be estimated using standard Strichartz theory. For the term $\mathcal{I}_7$, it follows from Proposition A.1(i) that for admissible pair $(q,r)$,

$$\left\|\mathcal{U}(t-s)\left(\psi_k - \frac{\langle\psi_j,\psi_k\rangle}{\langle\psi_j,\psi_j\rangle}\psi_j\right)\right\|_{L^q(\mathbb{R},L^r)} \le C\left\|\psi_k - \frac{\langle\psi_j,\psi_k\rangle}{\langle\psi_j,\psi_j\rangle}\psi_j\right\|_{L^2(\mathbb{R}^d)} \le 2C,$$

where we used $|\langle\psi_j,\psi_k\rangle| \le 1$. Hence,

$$\mathcal{I}_7 \le 2CT.$$

We denote the right-hand side of (A.2) as $\mathcal{S}[\psi_j](t)$. Then, we choose $T$ sufficiently small so that the map $\mathcal{S}$ becomes a strict contraction and finally use the standard fixed point theory to show the local existence for (A.1). □

We are now ready to present a proof of Theorem 3.1

**Proof of Theorem 3.1.** To extend the local solution to the global solution, we refine the energy estimate in Lemma 2.1. For the energy estimate, we assume that the solution $\{\psi_j\}_{j=1}^N$ is sufficiently regular so that the following estimates can be performed. We recall the simplified notation in (2.6):

$$C_j[\Psi] = \frac{1}{2}\sum_{\ell=1}^N \beta_{j\ell}|\psi_\ell|^2.$$

We observe

$$\begin{aligned}\sum_{j=1}^N \mathcal{E}_j^1[\Psi] &= \sum_{j=1}^N (V_j + C_j[\Psi])|\psi_j|^2 = \frac{2}{4}\left[\sum_{j=1}^N (V_j + C_j[\Psi])|\psi_j|^2 + \sum_{k=1}^N (V_k + C_k[\Psi])|\psi_k|^2\right], \\ \sum_{j=1}^N \mathcal{E}_j^2[\Psi] &= \frac{1}{4}\sum_{j,k=1}^N (V_j + V_k + C_j[\Psi] + C_k[\Psi])(|\psi_j|^2 + |\psi_k|^2).\end{aligned} \tag{A.3}$$

Then, $(\mathrm{A.3})_2$–$(\mathrm{A.3})_1$ yields

$$\begin{aligned}\sum_{j=1}^N \mathcal{E}_j^2[\Psi] - \sum_{j=1}^N \mathcal{E}_j^1[\Psi] &= \frac{1}{4}\sum_{j,k=1}^N (V_j - V_k + C_j[\Psi] - C_k[\Psi])(|\psi_j|^2 - |\psi_k|^2) \\ &\le \frac{1}{4}\sum_{j,k=1}^N (V_j + C_j[\Psi])|\psi_j|^2 + \frac{1}{4}\sum_{j,k=1}^N (V_k + C_k[\Psi])|\psi_k|^2 = \frac{N}{2}\sum_{j=1}^N \mathcal{E}_j^1[\Psi].\end{aligned} \tag{A.4}$$

We substitute the estimate (A.4) into (2.13) in Lemma 2.1 to obtain

$$\frac{d}{dt}\mathcal{E}[\Psi] = \kappa\sum_{j=1}^N \mathcal{E}_j^2[\Psi] - \kappa\sum_{j=1}^N r_j\mathcal{E}_j^1[\Psi] - \kappa\mathcal{E}_{\mathrm{d}}[\Psi] \le \kappa\left(1+\frac{N}{2}\right)\sum_{j=1}^N \mathcal{E}_j^1[\Psi] = \kappa\left(1+\frac{N}{2}\right)\mathcal{E}[\Psi]. \tag{A.5}$$

By integrating (A.5), we find

$$\mathcal{E}[\Psi](t) \le \mathcal{E}[\Psi](0)e^{\kappa\left(1+\frac{N}{2}\right)t}, \quad t\in[0,T]. \tag{A.6}$$

Hence, the energy does not blow up in any finite time interval. This completes the proof.

**Remark A.1.** In Sections 5.2 and 5.3, we impose a priori condition:

$$\sup_{0\le t\le T}\max_j \|\psi_j(t)\|_4 \le M(T) < \infty.$$

From the refined energy estimate (A.6), one has

$$\int_{\mathbb{R}^d}|\psi_j(x,t)|^4dx \le \frac{1}{\beta_{jj}}\mathcal{E}[\Psi] \le \frac{\mathcal{E}[\Psi](0)}{\beta_{jj}}e^{\kappa\left(1+\frac{N}{2}\right)t}, \quad j=1,\dots,N, \quad t\in[0,T].$$

## Appendix B. Proof of Lemma 4.3

Consider the first-order system with variable coefficients:

$$\begin{cases} \dot{Z}(t) = A(t)Z(t) + G(t), & t > 0, \\ Z(0) = (x^0, y^0). \end{cases}$$

where

$$Z(t) := \begin{pmatrix} x(t) \\ y(t) \end{pmatrix}, \quad A(t) := \begin{pmatrix} f(t) & p \\ -q & f(t) \end{pmatrix}, \quad G(t) := \begin{pmatrix} g_1(t) \\ g_2(t) \end{pmatrix}.$$

Then, our purpose is to derive a representation formula for the solution $Z(t) = (x(t), y(t))$:

$$\begin{aligned} \begin{pmatrix} x(t) \\ y(t) \end{pmatrix} &= \begin{pmatrix} e^{\int_0^t f(s)ds} & 0 \\ 0 & e^{\int_0^t f(s)ds} \end{pmatrix} \begin{pmatrix} \cos(\sqrt{pq}t) & \sqrt{\frac{p}{q}}\sin(\sqrt{pq}t) \\ -\sqrt{\frac{q}{p}}\sin(\sqrt{pq}t) & \cos(\sqrt{pq}t) \end{pmatrix} \begin{pmatrix} x^0 \\ y^0 \end{pmatrix} \\ &\quad + e^{\int_0^t A(s)ds} \int_0^t e^{-\int_0^s A(\tau)d\tau} G(s)ds, \quad t \geq 0. \end{aligned} \tag{B.1}$$

The derivation of (B.1) will be performed in two steps.

- Step A (Derivation of integral representation of $Z$): We set

$$F(t) := \int_0^t f(s)ds, \quad t > 0.$$

and claim:

$$A(t)\left(\int_0^t A(s)ds\right) = \left(\int_0^t A(s)ds\right)A(t), \quad t \geq 0. \tag{B.2}$$

For the proof of claim (B.2), note that

$$\begin{aligned} &A(t)\int_0^t A(s)ds \\ &= \begin{pmatrix} f(t) & p \\ -q & f(t) \end{pmatrix}\begin{pmatrix} F(t) & pt \\ -qt & F(t) \end{pmatrix} = \begin{pmatrix} f(t)F(t) - pqt & ptf(t) + pF(t) \\ -qF(t) - qtf(t) & -pqt + f(t)F(t) \end{pmatrix} \\ &= \begin{pmatrix} F(t) & pt \\ -qt & F(t) \end{pmatrix}\begin{pmatrix} f(t) & p \\ -q & f(t) \end{pmatrix} = \left(\int_0^t A(s)ds\right)A(t). \end{aligned}$$

This verifies our claim (B.2). Hence, we can use a variation of parameters to get

$$Z(t) = Z(0)e^{-\int_0^t A(s)ds} + e^{-\int_0^t A(s)ds}\int_0^t e^{\int_0^s A(\tau)d\tau} G(s)ds, \quad t \geq 0.$$

- Step B (Explicit calculation of $e^{\int_0^t A(s)ds}$): First note that

$$\int_0^t A(s)ds = \begin{pmatrix} F(t) & pt \\ -qt & F(t) \end{pmatrix} = \begin{pmatrix} F(t) & 0 \\ 0 & F(t) \end{pmatrix} + \begin{pmatrix} 0 & pt \\ -qt & 0 \end{pmatrix} =: B_1(t) + B_2(t).$$

By straightforward calculation, it is easy to see the commutativity of $B_1$ and $B_2$:

$$\begin{aligned} B_1(t)B_2(t) &= \begin{pmatrix} F(t) & 0 \\ 0 & F(t) \end{pmatrix}\begin{pmatrix} 0 & pt \\ -qt & 0 \end{pmatrix} = \begin{pmatrix} 0 & F(t)pt \\ -F(t)qt & 0 \end{pmatrix}, \\ B_2(t)B_1(t) &= \begin{pmatrix} 0 & pt \\ -qt & 0 \end{pmatrix}\begin{pmatrix} F(t) & 0 \\ 0 & F(t) \end{pmatrix} = \begin{pmatrix} 0 & F(t)pt \\ -F(t)qt & 0 \end{pmatrix}. \end{aligned}$$

Thus, we can see that $B_1(t)$ and $B_2(t)$ commute:

$$B_1(t)B_2(t) = B_2(t)B_1(t), \quad t \geq 0.$$

Hence, we can write

$$e^{\int_0^t A(s)ds} = e^{B_1(t)}e^{B_2(t)}. \tag{B.3}$$

To calculate $e^{\int_0^t A(s)ds}$, we present the estimate of $e^{B_1(t)}$ and $e^{B_2(t)}$, respectively.

◇ (Estimate of $e^{B_1(t)}$): Since $B_1(t)$ is a diagonal matrix, its matrix exponential is given by

$$e^{B_1(t)} = \begin{pmatrix} e^{F(t)} & 0 \\ 0 & e^{F(t)} \end{pmatrix}, \quad t \geq 0. \tag{B.4}$$

◇ (Estimate of $e^{B_2(t)}$): It follows from definition of matrix exponential and the identity

$$\big(B(t)\big)^2 = \big(-pqt^2\big)I_d, \quad t \geq 0$$

that one has

$$\begin{aligned} e^{B_2(t)} &= I_2 + B_2(t) + \frac{1}{2!}B_2(t)^2 + \frac{1}{3!}B_2(t)^3 + \frac{1}{4!}B_2(t)^4 + \cdots \\ &= \left(1 - \frac{pqt^2}{2!} + \frac{(pqt^2)^2}{4!} + \cdots\right) I_2 + \left(1 - \frac{pqt^2}{3!} + \frac{(pqt^2)^2}{5!} + \cdots\right) B_2(t) \\ &= \cos(\sqrt{pq}t)I_2 + \frac{\sin(\sqrt{pq}t)}{\sqrt{pq}t} B_2(t) \\ &= \begin{pmatrix} \cos(\sqrt{pq}t) & 0 \\ 0 & \cos(\sqrt{pq}t) \end{pmatrix} + \begin{pmatrix} 0 & \sqrt{\frac{p}{q}}\sin(\sqrt{pq}t) \\ -\sqrt{\frac{q}{p}}\sin(\sqrt{pq}t) & 0 \end{pmatrix} \\ &= \begin{pmatrix} \cos(\sqrt{pq}t) & \sqrt{\frac{p}{q}}\sin(\sqrt{pq}t) \\ -\sqrt{\frac{q}{p}}\sin(\sqrt{pq}t) & \cos(\sqrt{pq}t) \end{pmatrix}, \quad t \geq 0. \end{aligned} \tag{B.5}$$

In (B.3), we combine (B.4) and (B.5) to find

$$e^{\int_0^t A(s)ds} = \begin{pmatrix} e^{F(t)} & 0 \\ 0 & e^{F(t)} \end{pmatrix} \begin{pmatrix} \cos(\sqrt{pq}t) & \sqrt{\frac{p}{q}}\sin(\sqrt{pq}t) \\ -\sqrt{\frac{q}{p}}\sin(\sqrt{pq}t) & \cos(\sqrt{pq}t) \end{pmatrix}, \quad t \geq 0.$$

This completes the proof.

## References


[1] M.H. Anderson, J.R. Ensher, M.R. Matthewa, C.E. Wieman, E.A. Cornell, Observation of Bose–Einstein condensation in a dilute atomic vapor, Science 269 (1995) 198–201.
[2] C.C. Bradely, C.A. Sackett, J.J. Tollett, R.G. Hulet, Evidence of Bose–Einstein condensation in an atomic gas with attractive interaction, Phys. Rev. Lett. 75 (1995) 1687–1690.
[3] K.B. Davis, M.O. Mewes, N.J. Andrews, D.S. Drufee, D.M. Kurn, W. Ketterle, Bose–Einstein condensation in a gas of sodium atoms, Phys. Rev. Lett. 75 (1995) 3969–3973.
[4] E.P. Gross, Structure of a quantized vortex in boson systems, Nuovo Cimento 20 (1961) 454–457.
[5] L.P. Pitaevskii, Vortex lines in an imperfect Bose gas, J. Exp. Theor. Phys. 2 (1961) 451–454.
[6] W. Bao, Y. Cai, Mathematical theory and numerical methods for Bose–Einstein condensation, Kinet. Relat. Models 6 (2013) 1–135.
[7] X. Antoine, W. Bao, C. Besse, Computational methods for the dynamics of the nonlinear Schrödinger/Gross–Pitaevskii equations, Comput. Phys. Comm. 184 (2013) 2621–2633.
[8] W. Bao, Y. Cai, Uniform error estimates of finite difference methods for the nonlinear Schrödinger equation with wave operator, SIAM J. Numer. Anal. 50 (2012) 492–521.
[9] B. Guo, The convergence of numerical method for nonlinear Schrödinger equations, J. Comput. Math. 4 (1986) 121–130.
[10] W. Bao, Y. Cai, Mathematical models and numerical methods for spinor Bose–Einstein condensates, Commun. Comput. Phys. 24 (2018) 899–965.
[11] W. Bao, D. Jaksch, P.A. Markowich, Numerical solution of the Gross–Pitaevskii equation for Bose–Einstein condensation, J. Comput. Phys. 187 (2003) 318–342.
[12] W. Bao, S. Jin, P.A. Markowich, On time-splitting spectral apporximations for the Schrödinger equation in the semiclassical regime, J. Comput. Phys. 175 (2002) 487–524.
[13] W. Bao, S. Jin, P.A. Markowich, Numerical study of time-splitting spectral discretizations of nonlinear Schrödinger equations in the semiclassical regimes, SIAM J. Sci. Comput. 25 (2003) 27–64.
[14] W. Bao, Y. Zhang, Dynamics of the ground state and central vortex states in Bose–Einstein condensation, Math. Models Methods Appl. Sci. 15 (2005) 1863–1896.
[15] L.-M. Duan, B. Wang, H.J. Kimble, Robust quantum gates on neutral atoms with cavity-assisted photon scattering, Phys. Rev. A 72 (2005) 032333.
[16] G.L. Giorgi, F. Galve, G. Manzano, P. Colet, R. Zambrini, Quantum correlations and mutual synchronization, Phys. Rev. A 85 (2012) 052101.
[17] I. Goychuk, J. Casado-Pascual, M. Morillo, J. Lehmann, P. Hänggi, Quantum stochastic synchronization, Phys. Rev. Lett. 97 (2006) 210601.
[18] G. Heinrich, M. Ludwig, J. Qian, B. Kubala, F. Marquardt, Collective dynamics in optomechanical arrays, Phys. Rev. Lett. 107 (2011) 043603.
[19] H.J. Kimble, The quantum internet, Nature 453 (2008) 1023–1030.
[20] W. Li, L. Chong, S. Heshan, Quantum synchronization in an optomechanical system based on Lyapunov control, Phys. Rev. E 93 (2016) 062221.
[21] W. Li, L. Chong, S. Heshan, Quantum synchronization and quantum state sharing in an irregular complex network, Phys. Rev. E 95 (2017) 022204.
[22] M. Machida, T. Kano, S. Yamada, M. Okumura, T. Imamura, T. Koyama, Quantum synchronization effects in intrinsic josephson junctions, Physica C 468 (2008) 689–694.
[23] A. Mari, A. Farace, N. Didier, V. Giovannetti, R. Fazio, Measures of quantum synchronization in continuous variable systems, Phys. Rev. Lett. 111 (2013) 103605.
[24] V.M. Vinokur, T.I. Baturina, M.V. Fistul, A.Y. Mironov, M.R. Baklanov, C. Strunk, Superinsulator and quantum synchronization, Nature 452 (2008) 613–616.
[25] O.V. Zhirov, D.L. Shepelyansky, Quantum synchronization and entanglement of two qubits coupled to a driven dissipative resonator, Phys. Rev. B 80 (2009) 014519.
[26] O.V. Zhirov, D.L. Shepelyansky, Quantum synchronization, Eur. Phys. J. D 38 (2006) 375–379.

[27] B. Zhu, J. Schachenmayer, M. Xu, F. Herrera, J.G. Restrepo, M.J. Holland, A.M. Rey, Synchronization of interacting quantum dipoles, New J. Phys. 17 (2015) 083063.
[28] D. Witthaut, S. Wimberger, R. Burioni, M. Timme, Classical synchronization indicates persistent entanglement in isolated quantum systems, Nature Commun. 8 (2017) 14829.
[29] J.A. Acebron, L.L. Bonilla, C.J.P. Pérez Vicente, F. Ritort, R. Spigler, The Kuramoto model: a simple paradigm for synchronization phenomena, Rev. Modern Phys. 77 (2005) 137–185.
[30] S.-Y. Ha, D. Ko, J. Park, X. Zhang, Collective synchronization of classical and quantum oscillators, EMS Surv. Math. Sci. 3 (2016) 209–267.
[31] S.H. Strogatz, From Kuramoto to Crawford: Exploring the onset of synchronization in populations of coupled oscillators, Physica D 143 (2000) 1–20.
[32] T.E. Lee, H.R. Sadeghpour, Quantum synchronization of quantum van der Pol oscillators with trapped ions, Phys. Rev. Lett. 111 (2013) 234101.
[33] S. Walter, A. Nunnenkamp, C. Bruder, Quantum synchronization of two Van der Pol oscillators, Ann. Phys. 527 (2015) 131–138.
[34] P. Antonelli, S.-Y. Ha, D. Kim, P. Marcati, The Wigner-Lohe model for quantum synchronization and its emergent dynamics, Netw. Heterog. Media 12 (2017) 403–416.
[35] L. DeVille, Synchronization and stability for quantum Kuramoto, J. Stat. Phys. 174 (2019) 160–187.
[36] S.-Y. Ha, D. Ko, S.W. Ryoo, Emergent dynamics of a generalized Lohe model on some class of Lie groups, J. Stat. Phys. 168 (2017) 171–207.
[37] S.-Y. Ha, S.W. Ryoo, On the emergence and orbital stability of phase-locked states for the Lohe model, J. Stat. Phys. 163 (2016) 411–439.
[38] M.A. Lohe, Non-Abelian Kuramoto model and synchronization, J. Phys. A 42 (2009) 395101.
[39] P. Antonelli, P. Marcati, A model of synchronization over quantum networks, J. Phys. A 50 (2017) 315101.
[40] J. Cho, S.-H. Choi, S.-Y. Ha, Practical quantum synchronization for the Schrödinger-Lohe system, J. Phys. A 49 (2016) 205203.
[41] S.-H. Choi, S.-Y. Ha, Quantum synchronization of the Schrödinger-Lohe model, J. Phys. A 47 (2014) 355104.
[42] H. Huh, S.-Y. Ha, Dynamical system approach to synchronization of the coupled Schrödinger–Lohe system, Quart. Appl. Math. 75 (2017) 555–579.
[43] H. Huh, S.-Y. Ha, D. Kim, Emergent behaviors of the Schrödinger-Lohe model on cooperative-competitive networks, J. Differential Equations 12 (2017) 8295–8321.
[44] W. Bao, Ground states and dynamics of multicomponent Bose–Einstein condensates, Multiscale Model. Simul. 2 (2004) 210–236.
[45] W. Bao, Y. Cai, Ground states of two-component Bose–Einstein condensates with an internal atomic Josephson junction, East Asia J. Appl. Math. 1 (2010) 49–81.
[46] Y. Zhang, W. Bao, H. Li, Dynamics of rotating two-component Bose–Einstein condensates and its efficient computation, Physica D 234 (2007) 49–69.
[47] W. Bao, Y. Cai, Ground states and dynamics of spin–orbit coupled Bose–Einstein condensates, SIAM J. Appl. Math. 2 (2015) 492–517.
[48] S.-Y. Ha, D. Kim, Emergence of synchronous behaviors for the Schrödinger-Lohe model with frustration, to appear in Nonlinearity.
[49] H. Huh, S.-Y. Ha, D. Kim, Asymptotic behavior and stability for the Schrödinger-Lohe model, J. Math. Phys. 59 (2018) 102701.
[50] M.A. Lohe, Quantum synchronization over quantum networks, J. Phys. A 43 (2010) 465301.
[51] Y. Kuramoto, Self-entrainment of a population of coupled non-linear oscillators, in: International Symposium on Mathematical Problems in Mathematical Physics, in: Lecture Notes in Theoretical Physics, vol. 30, 1975, pp. 420–422.
[52] Y.-P. Choi, S.-Y. Ha, S. Jung, Y. Kim, Asymptotic formation and orbital stability of phase-locked states for the Kuramoto model, Physica D 241 (2012) 735–754.
[53] X. Antoine, R. Duboscq, Robust and efficient preconditioned Krylov spectral solvers for computing the ground states of fast rotating and strongly interacting Bose–Einstein condensates, J. Comput. Phys. 258 (2014) 509–523.
[54] W. Bao, I. Chern, F. Lim, Efficient and spectrally accurate numerical methods for computing ground and first excited states in Bose–Einstein condensates, J. Comput. Phys. 219 (2006) 836–854.
[55] D. Kim, Q. Tang, On the numerical methods to simulate the dynamics of Gross–Pitaevskii-Lohe system and beyond, in preparation.
[56] T. Cazenave, Semilinear Schrödinger Equations, in: Courant Lecture Notes in Mathematics, vol. 10, New York University, Courant Institute of Mathematical Sciences, AMS, 2003.